10-4-2018 9:30 AM

The Effect of Anoxia on Mitochondrial Function in a Hibernator (Ictidomys tridecemlineatus)

Leah Hayward, *The University of Western Ontario*

Supervisor: Staples, James F., *The University of Western Ontario*

A thesis submitted in partial fulfillment of the requirements for the Master of Science degree in Biology

ABSTRACT

Hibernation protects mammalian tissues against ischemia-reperfusion injury, but the underlying biochemical mechanisms are unknown. I hypothesized that the mechanisms allowing for mitochondrial metabolic flexibility during hibernation permit anoxia tolerance and contribute to tissue ischemia-reperfusion tolerance. I assessed mitochondrial performance before and after five minutes of anoxia in liver mitochondria isolated from thirteen-lined ground squirrels. I compared this anoxia effect among animals that were summer active (SA), or during hibernation (in torpor or interbout euthermia; IBE). Anoxia decreased state 3 respiration in all groups, but mitochondria isolated from torpid squirrels were least affected; these decreases paralleled decreased activity of electron transport system complexes in IBE and SA. Leak respiration was more elevated in SA mitochondria following anoxia than in either IBE or torpor. These findings suggest that during hibernation (especially in torpor) mitochondrial respiration is maintained with a concurrent reduction in oxidative damage following anoxia, which may protect from ischemia-reperfusion injury.

Keywords: ischemia, reperfusion, hibernation, metabolism, thirteen-lined ground squirrel, high-resolution respirometry

CO-AUTHORSHIP STATEMENT

This thesis will be submitted in a modified form to the American Journal of Physiology, with Drs. Katherine E. Mathers and James F. Staples as co-authors. I produced all data contained within the thesis except Dr. Mathers performed spectrophotometric enzyme assays (p.32) and created figure 1-2. I contributed to experimental concept and design, analyzed data, and wrote the manuscript. Dr. Staples contributed to the experimental concept and design, as well as manuscript editing.

ACKNOWLEDGEMENTS

I would firstly like to thank my supervisor, Dr. Jim Staples, for his overwhelming support throughout this project. His constant guidance and trust in me has made this experience so rewarding, and I could not have asked for a better mentor. Thank you for all of the opportunities you gave me to share my work, see the world, and become a better scientist too.

Secondly, I would like to thank the members of my advisory committee, Drs. Chris Guglielmo and Rob Cumming. Their advice, expertise, and support kept me on track and challenged me to improve my project, and my skills as a researcher. I would also like to thank Dr. Ben Rubin for his help with the statistical analyses of these data.

Kate Mathers, thank you for your constant support, for always lending a helping hand, and for teaching me about all things bioenergetic – which was required often. You are the most selfless scientist and I really appreciate everything you did to make my life easier (and my figures nicer!). Amanda MacCannell, thank you for keeping me grounded throughout this entire process. I am so grateful for your continual encouragement and support, for always reminding me of my deadlines, but most of all for your friendship.

I must also thank Miya Wang and Maria Li for their help with squirrel care, as well as Sharla Thompson for her patience, generosity, and assistance with our (many) squirrel-related needs…I am glad the squirrels are in the most capable hands!

Thank you to my family (and Natasha) for your unwavering support in the pursuit of my goals. Your confidence in my abilities helped me to overcome every hurdle throughout this process, and your patience and generosity made the experience so much easier. To my fiancé Billy, thank you for your excitement on the good days, and for your encouragement on the bad days. Thank you for being my greatest friend and support, and for always keeping me well-caffeinated. I am so grateful for you, and this achievement is as much yours as it is mine. I love you all.

Lastly, thank you to NSERC, and the Ontario Graduate Scholarship Program for funding and supporting this research.

TABLE OF CONTENTS

LIST OF FIGURES

LIST OF APPENDICES

LIST OF ABBREVIATIONS AND SYMBOLS

$\Delta\psi_m$	membrane potential
A/R	anoxia/reoxygenation
ADP	adenosine 5'-diphosphate
ANT	adenine nucleotide translocase
ATP	adenosine triphosphate
BMR	basal metabolic rate
BSA	bovine serum albumin
CCCP	carbonyl cyanide *m*-chlorophenyl hydrazone
ETS	electron transport system
GPx4	glutathione peroxidase 4
GSH	reduced glutathione
GSSG	oxidized glutathione
HB	homogenization buffer
IBE	interbout euthermia
IMM	inner mitochondrial membrane
IMS	intermembrane space
I/R	ischemia/reperfusion
LDH	lactate dehydrogenase

Mt	mitochondria
MnSOD	manganese superoxide dismutase
$O_2^{\bullet}$	superoxide
Δp	protonmotive force
RCR	respiratory control ratio
ROS	reactive oxygen species
SA	summer active
ST3	state 3 respiration
ST4	state 4 respiration
T	torpor
T_a	ambient temperature
T_b	body temperature
TBS-T	tris-buffered saline
TCA	tricarboxylic acid
TPP	tetraphenylphosphonium
TNZ	thermoneutral zone
UCP	uncoupling protein

CHAPTER 1

1 INTRODUCTION

1.1 The cost of endothermy

Maintenance of energy homeostasis is vital to any organism's survival, and is therefore under strong selective pressure. Ambient temperature (T_a) is one abiotic factor that affects an animal's energy metabolism. Ectothermic animals have body temperatures (T_b) that are largely determined by environmental temperatures, which affect the rate of biochemical processes needed to generate ATP. Endothermic animals, such as mammals and birds, instead rely on endogenously-derived heat to maintain T_b across a broad range of T_a, which allows such animals to thrive in colder climates. Decreases in T_a necessitate elevated energy demand for effective thermoregulation, and as a consequence, endotherms have basal metabolic rates (BMR) that are 5-15 times higher than similar-sized ectotherms (40, 85).

Endotherms can sustain normothermia within a narrow range of ambient temperatures without requiring increasing metabolic rate. This T_a range is called the thermoneutral zone (TNZ), and T_b is regulated within the TNZ through postural changes, constriction or dilation of peripheral blood vessels, or piloerection, all of which require very little metabolic energy. At temperatures outside of the TNZ, increases in metabolic demand are required to support active heat production or heat dissipation. This thermoregulatory demand can be a challenge for small endotherms in stressful environments, where the availability of resources needed to power thermogenesis may be low. For example, despite a lower partial pressure of O_2 at high altitude, high altitude deer mice (*Peromyscus maniculatus*) have 57% higher mass-specific field metabolic rates (FMR) than low altitude conspecifics (37), which is necessary for thermoregulation at colder T_a. As a result, high altitude mice operate closer to their maximal aerobic capacity and have lower aerobic scopes (37). A higher FMR is likely attributable to low food availability (therefore greater foraging effort) and high thermogenic demand at high altitude (37).

Environmental stressors, such as those at high altitude or latitude, shape the thermal and energetic strategies of small endotherms. There are many diverse strategies that small endotherms employ to maintain T_b in stressful conditions such as increases in the capacity for non-shivering thermogenesis, or decreased thermal conductance. Heterothermy is likely the most complex strategy, as it involves coordinated adjustments to thermoregulation, metabolism, and other physiological systems. Most endotherms are homeothermic and use internal heat production to maintain a stable core T_b determined by a thermoregulatory set-point (T_{set}). In eutherian mammals, T_{set} is typically near 37°C. The ability of heterothermic endotherms to decrease T_{set} significantly reduces energy demand, which is especially beneficial in environments that are resource-limited. Torpor is defined as a regulated depression of metabolic rate, and therefore T_b. Some endotherms use torpor, during which T_{set} is reduced in a regulated fashion, to reduce the demand for metabolic heat production. Torpor is also commonly referred to as heterothermy, or daily heterothermy in species that experience torpor bouts lasting less than one day (85). In the white-footed mouse (*Peromyscus leucopus*) five hours of daily torpor, with a maximal reduction of T_b by 15°C, decreases daily energy expenditure by up to 22% (87). Hibernation involves periods of torpor that last longer than one day, and is typically associated with greater reductions in metabolic rate and T_b.

1.2 Hibernation physiology

Hibernation is defined as a seasonal, regulated suppression of metabolic rate to less than 10% of euthermic rates, followed by a reduction in T_b (77). It is estimated that hibernation is associated with energy savings of up to 90% in some species (85). Such significant reductions in metabolic rate reduce the energy costs of thermoregulation in cold environments. Small hibernators, such as the 13-lined ground squirrel (*Ictidomys tridecemlineatus*) spend most of the hibernation season in a torpid state, where metabolic rate is reduced by up to 95% and T_b declines to 5°C. These torpor bouts are interrupted by spontaneous arousals, where both metabolic rate and T_b return to euthermic levels for several hours (interbout euthermia; IBE) before entrance back into torpor (Figure 1-1A; ref. 76). Torpor is also characterized by a decrease in heart rate, blood pressure, blood flow, and ventilation rate relative to IBE (67, 77), so rapid arousals from torpor are often

thought to cause transient mismatches between oxygen supply and demand, which mimics pathological conditions such as ischemia-reperfusion in certain tissues (Figure 1-1B; reviewed in ref. 77). As cardiac output increases before metabolic rate during an arousal, tissues with increasing metabolic demand during arousal are likely not oxygen-limited. However, blood flow to peripheral organs (such as the kidneys, liver, spleen, and gut) is restricted during torpor and into late-arousal (when thoracic T_b reaches 25°C) compared to heart, diaphragm, and brown adipose tissue (15), which could restrict O_2 supply to these tissues and have damaging effects.

A decrease in O_2 supply to tissues limits the capacity to produce ATP by oxidative phosphorylation. Depending on the severity and length of O_2 deprivation, cells may become exclusively reliant on glycolysis for ATP generation. Increased reliance on glycolysis can cause cellular acidification and rapid substrate depletion, which can lead to a decline in [ATP] and compromise ATP-dependent cellular processes (88, explained in Section 1.5.3). Subsequent to O_2 restriction, re-oxygenation of a previously hypoxic tissue can lead to elevated reactive oxygen species (ROS) formation, which can cause widespread damage to proteins, lipids, and DNA (explained in Section 1.5.2). This pathological event is analogous to ischemia-reperfusion (I/R) injury, which occurs when blood supply (and likely O_2) to tissues is restricted and subsequently restored, as during an ischemic stroke. Because hibernators routinely experience periodic reductions and restorations of blood flow during the winter, they have been used as models of resistance to I/R injury.

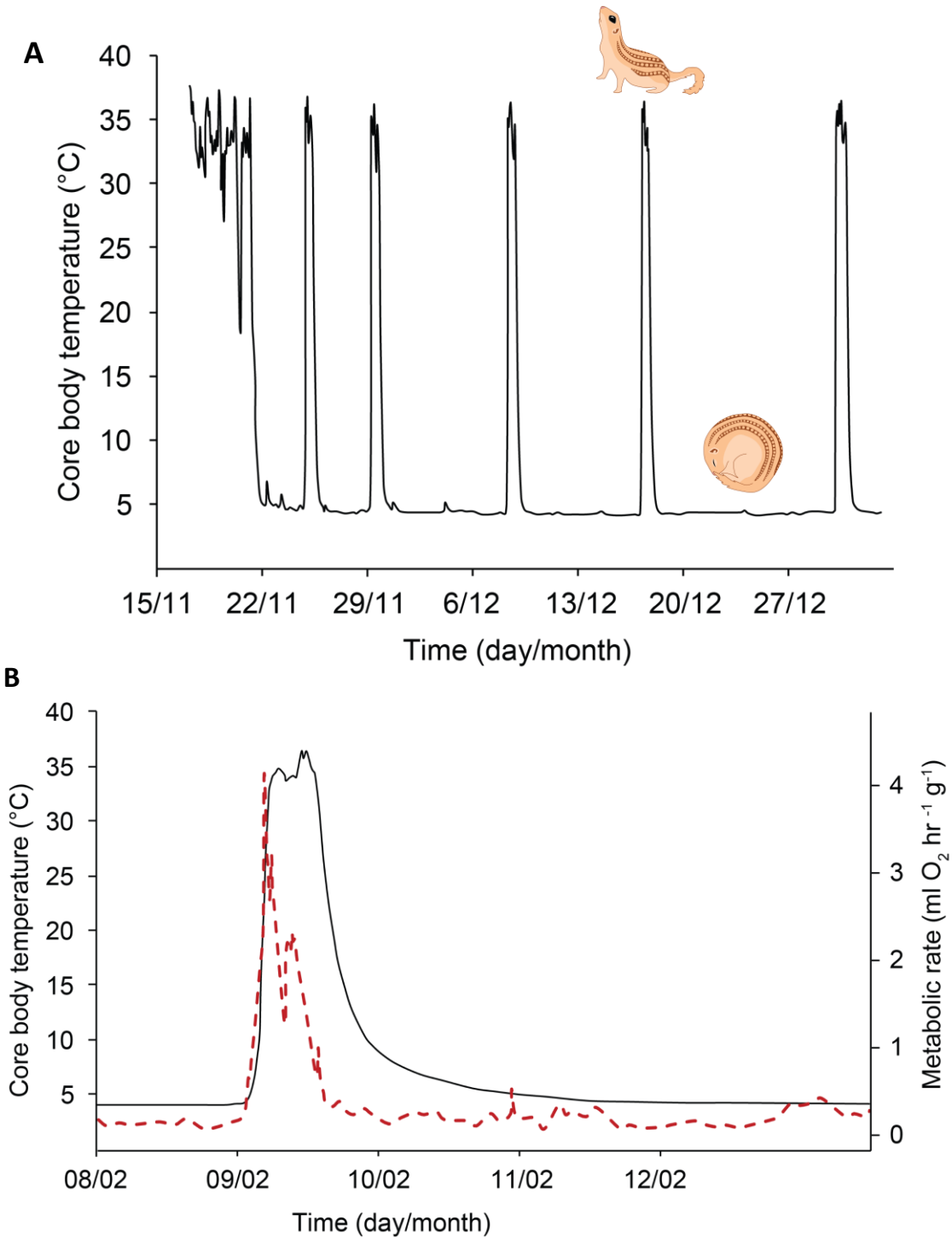

Figure 1-1. Torpor-arousal cycles in the 13-lined ground squirrel. Core body temperature cycles between two extremes (5°C and 37°C) over the hibernation season (A), and metabolic rate (in red) increases rapidly during arousal from torpor, preceding increases in T_b (B), which is thought to cause transient hypoxia in peripheral tissues (modified from ref. 76).

1.3 Evidence for oxidative stress during hibernation

Whether oxidative stress occurs during arousal from torpor is under debate, and is likely tissue-specific. Plasma or tissue-level antioxidant dynamics have often been studied to explore this contentious topic. For example, the rapid decline of ascorbate (an antioxidant produced by the liver) in the plasma of arousing Arctic ground squirrels (*Spermophilus parryii*) coincides with maximal oxygen consumption during arousal (82). As maximal oxygen consumption presumably correlates with reperfusion of major organs, ascorbate clearance from plasma and uptake by tissues (such as the liver) is suggested to serve a protective role against oxidative damage. Additionally, urate (a marker of ROS production) increases in aroused *S. parryii* liver relative to torpor (82). In the intestinal mucosa of 13-lined ground squirrels, the ratio of reduced glutathione (GSH) to oxidized glutathione (GSSG) is lower in hibernation compared to euthermia, suggesting that oxidative stress increases in torpor (18). Also, upregulation of the mitochondrial stress protein GRP75 occurs during the hibernation season in the intestine of 13-lined ground squirrels, which further indicates that torpor is associated with oxidative stress (17).

Despite these findings, there is no evidence for increased levels of lactate, the end product of glycolysis under hypoxic conditions, within the liver during torpor or entrance into torpor in 13-lined ground squirrels (72), and plasma lactate levels are similar in torpor to mid- and late-arousal levels in the AGS (51), which challenges the idea that hibernation is associated with hypoxia. Additionally, there are no increases in either the activity or expression of important antioxidants (mitochondrial or cellular superoxide dismutase, glutathione peroxidase, or glutathione reductase) in major oxidative tissues of 13-lined ground squirrels during hibernation (59). Taking all of these studies together, it is not clear whether hibernators entirely avoid oxidative stress during the transition from torpor to IBE, or whether hibernation provides some protection against oxidative damage. Despite this knowledge gap, hibernator tissues are more hypoxia tolerant than those from non-hibernators (25), and this tolerance improves during the hibernation season (46, 49).

1.4 Hypoxia tolerance in vertebrates

1.4.1 Metabolic suppression as a unifying feature of hypoxia tolerance

Hypoxia tolerance in mammals and ectothermic vertebrates is often associated with regulated metabolic suppression (84). In diving mammals, metabolic suppression corresponds with tissue hypoperfusion in both liver and kidney (41). Interestingly, mammalian neonatal hypoxia resistance involves strategies common to both diving mammals and mammalian hibernators: neonates can endure low partial pressures of oxygen *in utero* and during birth asphyxia through a combination of reduced metabolic rate, body temperature, and blood flow to peripheral organs and tissues (75). Naked mole rats, fossorial mammals that experience chronic hypoxia in their burrows, can survive complete anoxia by reducing energy demand and switching to fructose-supported anaerobic metabolism (61). There are some ectothermic vertebrates, such as North American freshwater turtles and Eurasian cyprinid fishes, that tolerate complete anoxia while overwintering naturally in ice-covered water bodies (78). These animals also exhibit profound suppression of both metabolic rate and body temperature, and have mechanisms to avoid the build-up of anaerobic end products, such as lactate and H^+, in their blood (78). Since the T_b of ectotherms depends primarily on their environment, ectotherms have significantly lower ATP demands than similar-sized endotherms. This, combined with additional metabolic suppression, contributes to an ectotherm's ability to survive long periods in conditions that only support anaerobic glycolysis.

1.4.2 Hibernation and tolerance to ischemia/reperfusion

Although it is unknown whether hibernators experience hypoxia *in situ* at any point during the hibernation season, several hibernator tissues are known to tolerate ischemia-reperfusion. The mucosal tissue of the small intestine is significantly compromised following total occlusion and subsequent reperfusion of the superior mesenteric artery (which supplies blood to the intestines) in rats and summer-active 13-lined ground squirrels, but not in euthermic squirrels during an arousal (46). Livers isolated from 13-lined ground squirrels during the hibernation season retain hepatocellular function (measured as LDH release) and mitochondrial integrity (measured as respiratory control

ratio; RCR) following 72h of cold storage and reperfusion better than livers isolated from summer-active squirrels. Livers isolated from summer-active squirrels are less affected by cold storage and reperfusion than those isolated from rats, demonstrating that protection from I/R is specific to hibernators. Moreover, this damage-resistant phenotype appears to be enhanced during the hibernation season (49). Similarly, neurons in three regions of euthermic summer-active AGS brains (hippocampal, cortical, and striatal) demonstrate complete protection from induced cardiac arrest (CA) and subsequent resuscitation compared to rats (25).

It is unlikely that hypoxia tolerance in hibernators is a direct consequence of low T_b or metabolic suppression alone, since euthermic squirrels are tolerant to models of ischemia and reperfusion both during the hibernation season (in torpor and IBE, ref. 49) and in the summer (25). However, it is clear that the ability to suppress metabolism is a unifying feature of hypoxia-tolerant animals. To achieve substantial metabolic suppression, regulation at the mitochondrial level is necessary.

1.5 Mitochondrial physiology

In typical environments, mitochondria generate ATP through oxidative phosphorylation, which involves a series of redox reactions along the electron transport system (ETS). The ETS is comprised of six electron-transporting proteins embedded in the inner mitochondrial membrane (IMM). These proteins (protein complexes I through IV, ubiquinone, and cytochrome c) form a decreasing energy potential gradient along the IMM, which permits the flow of electrons from complex I to complex IV (54). The energy released from these sequential redox reactions is used to pump protons (H^+) from the mitochondrial matrix to the intermembrane space (IMS; between the IMM and outer mitochondrial membrane) through complexes I, III, and IV (54). The movement of protons from the matrix to the IMS establishes an electrochemical gradient (the protonmotive force; Δp) across the IMM. When ATP synthase (complex V) is stimulated, protons re-enter the matrix through the core of complex V which spans the IMM, powering ATP synthesis from ADP. ATP production (and therefore Δp dissipation) stimulates ETS flux and oxygen consumption at complex IV, where oxygen acts as the

final electron acceptor and combines with protons and electrons to form water. The maximal physiological rate of oxygen consumption coupled to ATP production is called state 3 respiration (ST3). However, there is a small amount of oxygen consumed at complex IV even in the absence of ATP production. This so-called state 4 respiration (ST4) ensures adequate electron flux (and therefore proton translocation from the matrix to the IMS) to compensate for inherent mitochondrial proton leak, which allows protons to move from the IMS to the matrix, while bypassing ATP synthase. A summary of normal ETS function is given in Figure 1-2.

1.5.1 Changes to mitochondrial metabolism during hibernation

To achieve substantial metabolic suppression in torpor, decreases in both ATP demand and production are necessary in a manner that is rapid and reversible. Mitochondrial metabolic suppression occurs in several hibernator tissues, and likely contributes significantly to whole animal reductions in MR during torpor (77). For example, liver mitochondria isolated from torpid ground squirrels exhibit a 60% reduction in succinate-linked ST3 relative to IBE and summer euthermic mitochondria (53). Reductions in ST3 respiration are paralleled by reductions in maximal complex I and II activity in torpor (53). In the liver, differential phosphorylation of ETS enzymes suggests that post-translational modifications may provide a mechanism for reversible metabolic suppression in torpor (52).

1.5.2 Reactive oxygen species: a consequence of mitochondrial respiration

In normally functioning mitochondria, a small proportion of electrons (0.1-0.5%) moving through the ETS participate in the uncatalyzed single or double reduction of O_2, forming superoxide ($O_2^{\bullet}$) or hydrogen peroxide (H_2O_2), respectively (8). Superoxide can damage proteins in the tricarboxylic acid (TCA) cycle (limiting ATP production; ref. 65) and can lead to the formation of other reactive species (such as hydroxyl, $HO^{\bullet}$, or hydroperoxyl, $HO_2^{\bullet}$) which can cause more widespread damage (54). The mechanism and extent of ROS-induced damage depends largely on bioenergetic state, the mitochondrial or cellular environment, and the context in which ROS are being produced (55). Proteins, lipids, and nucleic acids can all be damaged by oxidation. Specific mechanisms of damage include

the formation of reactive protein carbonyls, lipid peroxides or peroxyl radicals, and 8-hydroxydeoxyguanosine base formation in mitochondrial DNA (55, 57).

Superoxide and hydrogen peroxide are generated at 11 known sites along the ETS, and the contribution of each site to ROS production depends on the bioenergetic condition of the cell (90). ROS production depends on Δp because of the relationship between Δp and electron transfer. Due to mass action effects, a high Δp slows electron transfer through the ETS, which leads to increased electron leakage and the reduction of O_2 (54). A decrease in Δp occurs in all mitochondria in the presence of ADP during oxidative phosphorylation as a consequence of protons moving from the IMS to the matrix through ATP synthase (as described above in Section 1.5). Apart from oxidative phosphorylation, decreases in Δp are associated with mild uncoupling of ATP production from O_2 consumption, which allows proton re-entry into the matrix that is independent of ATP synthase and ATP production. Such uncoupling is associated with decreased ROS production (54) and can be achieved pharmacologically with amphipathic molecules such as carbonyl cyanide *m*-chlorophenyl hydrazone (CCCP). In a more physiologically-relevant context, slight dissipation of Δp can be facilitated by uncoupling proteins (UCPs), which can be activated by the products of lipid peroxidation (10).

Beyond limiting ROS production through uncoupling, cells can mitigate ROS propagation and damage using antioxidants. There are many antioxidant systems in the mitochondria that detoxify reactive oxygen species: manganese-dependent superoxide dismutase (MnSOD) converts $O_2^{\bullet}$ to H_2O_2, and H_2O_2 is catalyzed to H_2O primarily by glutathione peroxidase, peroxiredoxin, and thioredoxin systems (8). There are also two main non-enzymatic mitochondrial antioxidants. Vitamin E is localized to the IMM and limits the propagation of lipid peroxidation (36), and Vitamin C (ascorbate) is an antioxidant specific to the aqueous phase of the mitochondria, which can also regenerate Vitamin E that has been oxidized (28). High mitochondrial antioxidant capacity has been implicated in models of hypoxia tolerance in cancer cells (48), and several hypoxia-tolerant animals express high levels of antioxidants either constitutively, or prior to oxidative stress events (reviewed in refs. 6, 38).

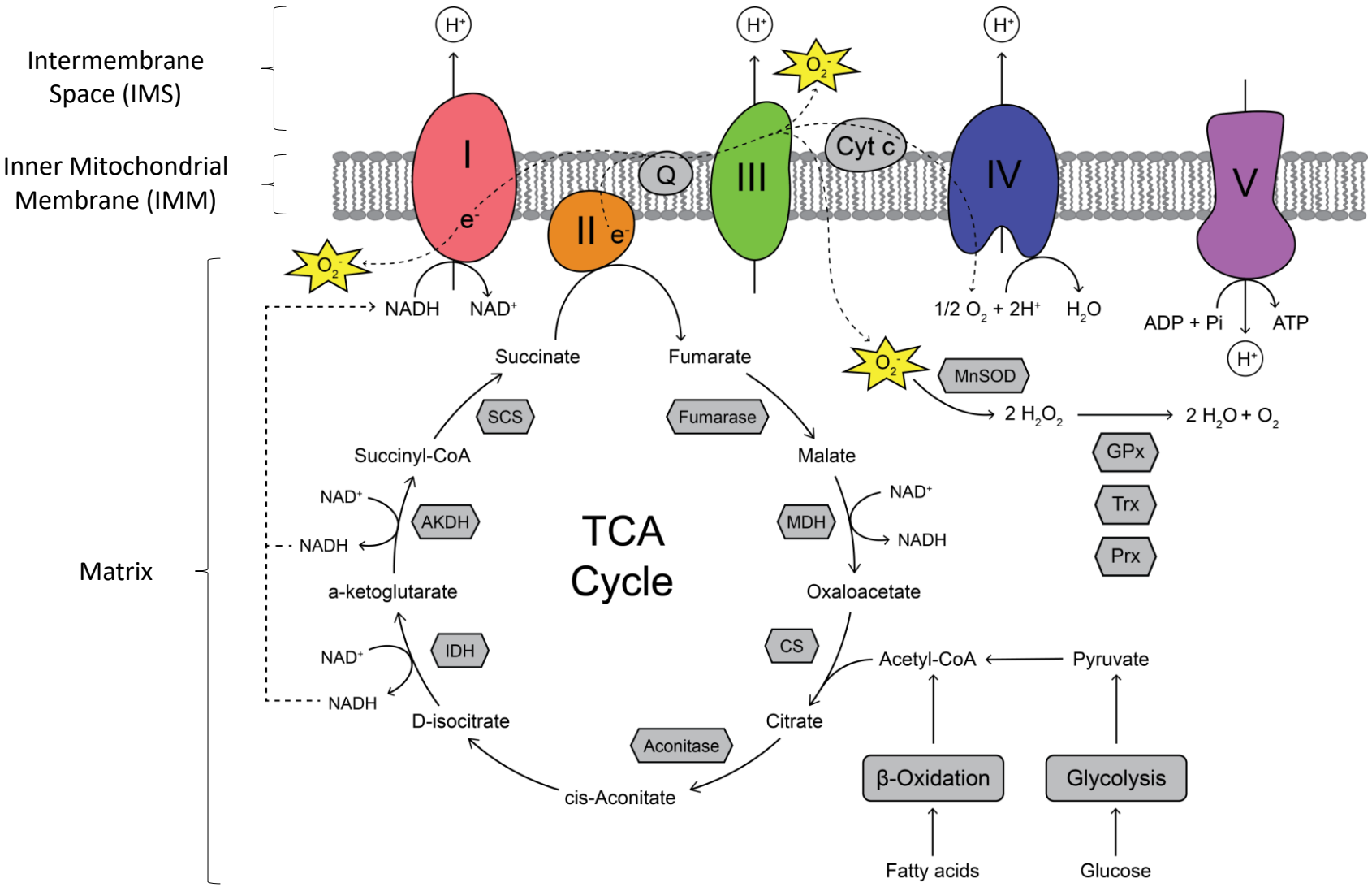
Intermembrane Space (IMS)
Inner Mitochondrial Membrane (IMM)
Matrix
H+
I
II
III
IV
V
Q
Cyt c
e-
O2-
NADH
NAD+
1/2 O2 + 2H+
H2O
ADP + Pi
ATP
Succinate
Fumarate
Succinyl-CoA
Malate
Oxaloacetate
Acetyl-CoA
Pyruvate
Citrate
cis-Aconitate
D-isocitrate
a-ketoglutarate
SCS
Fumarase
MDH
CS
Aconitase
IDH
AKDH
TCA Cycle
MnSOD
2 H2O2
2 H2O + O2
GPx
Trx
Prx
β-Oxidation
Glycolysis
Fatty acids
Glucose

Figure 1-2. Mitochondrial bioenergetics (p.10 above). NADH and succinate, derived from the tricarboxylic acid (TCA) cycle, donate electrons to complexes I and II of the electron transport system (ETS). Electrons move through the ETS through a series of redox reactions, down an energy potential gradient to complex IV, where they combine with O_2 and protons (H^+) to form H_2O. The energy released from these redox reactions is used to pump H^+ from the matrix to the intermembrane space (IMS) to generate a protonmotive force (Δp) across the inner mitochondrial membrane (IMM). This Δp is used to drive ATP synthesis through complex V in the presence of ADP (ST3), but is also dissipated through basal H^+ leak from the IMS to the matrix independently of ATP synthesis (leak respiration; ST4). Reactive oxygen species (ROS; $O2^{\bullet}$, H_2O_2) production is a normal byproduct of oxidative phosphorylation. However, mitochondrial ROS are detoxified by the antioxidant enzymes manganese-dependent superoxide dismutase (MnSOD), thioredoxin (Trx), peroxiredoxin (Prx), and glutathione peroxidase (GPx).

1.5.3 Typical mitochondrial response to hypoxia (and re-oxygenation)

Most damaging effects of hypoxia result from initial decreases in ATP supply (8). The cascade of events initiated by ischemia (which limits O_2 supply) and leading to cell apoptosis are summarized in Figure 1-3 (and comprehensively reviewed in refs. 50 and 7). Because O_2 (a substrate for complex IV) is limited in hypoxia, electron flux through the ETS slows and can eventually come to a halt in complete anoxia. Without sufficient electron flux, a loss of Δp occurs, which limits ATP synthesis through ATP synthase. Loss of ATP-generating capacity in the absence of sufficient oxygen limits ATP-dependent processes, such as maintenance of plasma membrane potential or ion homeostasis. Plasma membrane depolarization and loss of ion homeostasis (specifically Na^+ and Ca^{2+} homeostasis) can have catastrophic effects on the cell including cytoskeletal damage and ultimately cell death (30, 50). Although the initial hypoxic insult may not result in significant cell damage, re-oxygenation and re-establishment of oxidative phosphorylation triggers ROS formation and mitochondrial Ca^{2+} sequestration, which can lead to permeability transition pore (PT pore) opening and cell death (88).

The mitochondrial ETS is also implicated in ischemia-reperfusion damage because of its role in ROS generation, which occurs as a direct consequence of the redox state of electron carriers (66). As the duration of ischemia increases, oxygen becomes limiting. This alters the state of the ETS because the halting of electron flow shifts electron carriers to a more reduced state (16). Upon reperfusion, the combination of a rapid increase in local O_2 concentration and a high concentration of reduced electron-carriers results in a burst of mitochondrial ROS production. In mammalian models of ischemia-reperfusion, this burst of ROS typically exceeds the capacity of endogenous antioxidants and leads to oxidative tissue damage (18, 65).

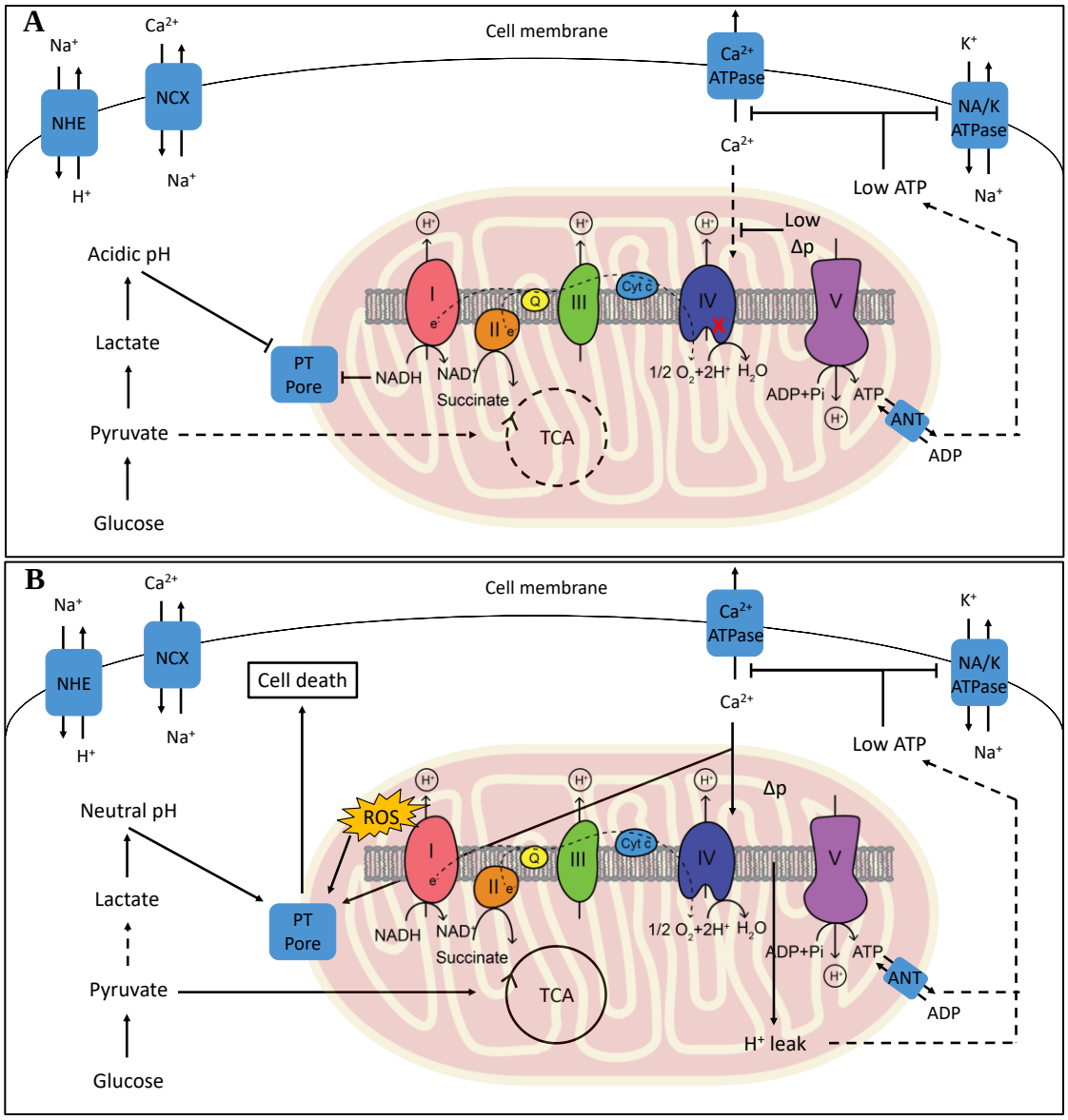

Figure 1-3. The effect of ischemia (A) and reperfusion (B) on cellular function. During ischemia (A), oxidative phosphorylation decreases, and ATP-dependent processes rely on glycolysis for ATP. This leads to acidification of the cytoplasm, Ca^{2+} overload, and loss of ion homeostasis if ischemia persists. During reperfusion (B), the rapid increase in local [O_2] combined with reduced electron carriers leads to ROS production. This in addition to restoration of neutral cytoplasmic pH and mitochondrial membrane potential (and therefore mitochondrial Ca^{2+} uptake) leads to PT pore opening and can ultimately cause cell death if ion homeostasis cannot be regained. Figure adapted from (88). Also see (7) and (50) for an overview of cellular function in ischemia. NHE=sodium-proton exchanger, NCX=sodium-calcium exchanger, Na/K-ATPase=sodium-potassium pump, Ca^{2+}-ATPase= calcium pump, ANT=adenine nucleotide translocator.

1.5.4 Hypoxia tolerance at the mitochondrial level

Mitochondrial dysfunction is associated with I/R pathology in humans. As such, pharmacological targets for preventing cell death following ischemia typically converge on mitochondrial components, such as ATP-dependent potassium channels (mK_{ATP}) or H^+ channels (88). These targets are likely implicated in processes that affect ROS production and Ca^{2+} overload (88). Since I/R-related damage occurs largely as a consequence of ATP loss and ROS production at the mitochondrial level, the question that remains is: How do anoxia-tolerant organisms avoid these pathological consequences of O_2 deprivation?

Hypoxia-tolerant organisms possess mitochondria that are also hypoxia-tolerant *in vitro*, but the mechanisms that confer this tolerance are unknown. Heart fibres isolated from the hypoxia-tolerant epaulette shark (*Hemiscyllum ocellatum*) maintain a higher mitochondrial coupling efficiency (RCR) and lower ROS production rates than heart fibres isolated from the hypoxia-sensitive shovelnose ray (*Aptychotrema rostrate*) following *in vivo* hypoxic exposure. The epaulette shark is able to limit ATP depletion (through maintenance of ETS efficiency) and ROS production after hypoxia and re-oxygenation, which likely contributes to its superior hypoxia tolerance (39). After two weeks of chronic anoxia, heart mitochondria isolated from turtles (*Trachemys scripta*) maintain maximal respiration rates after being subjected to anoxia/reoxygenation *in vitro*. The maximal respiration rate of cardiac fibres was lower after chronic anoxia compared to normoxic turtles, and this reduction in ATP demand was achieved by significant inhibition of complex V (29).

1.6 Objectives and hypothesis

It is well established that hibernator tissues are more hypoxia tolerant than non-hibernator tissues, perhaps related to insufficient blood flow to peripheral organs during arousal from torpor. Since metabolic suppression is a unifying characteristic of hypoxia-tolerant organisms, and regulated metabolic suppression occurs in torpid liver mitochondria, I hypothesized that the mechanisms allowing for metabolic suppression during hibernation also permit anoxia tolerance. I predicted that liver mitochondria isolated from 13-lined

ground squirrels during torpor would be more anoxia-tolerant than mitochondria from IBE or summer active (SA) squirrels. To test this prediction, I measured characteristics of mitochondrial metabolism before and after anoxia, and compared the anoxic effect among animals that were in torpor, IBE, or SA.

My first objective was to determine the effect of anoxia on three mitochondrial performance metrics: (1) maximal ADP-stimulated respiration (i.e. ST3); (2) leak respiration (i.e. ST4); and (3) membrane potential (the main contributor to Δp). My second objective was to determine whether any differences in these metrics could be explained by differences in antioxidant expression, or changes to the maximal enzyme activity of three ETS complexes (complexes I, II, and V).

CHAPTER 2

2 METHODS

2.1 Experimental animals

All experiments were performed in accordance with the Western University Animal Care Protocol (2012-016) and following guidelines from the Canadian Council on Animal Care (Appendix 1).

The 13-lined ground squirrels (*Ictidomys tridecemlineatus*) used in this study were either live-trapped in Carman, MB (49°30'N, 98°01'W) in either June 2016 or May 2017 under Manitoba Conservation collection permit number WB18908, or born in captivity following established husbandry protocols (86). Animals were provided with food (Prolab Isopro RMH 3000, Lab Diet, St. Louis, MO) and water *ad libitum* and housed at 23°C from April to November 2017 with a photoperiod matching that of Carman, MB, which was adjusted weekly. Animals were moved to an environmental chamber in November, where the temperature was lowered by 1°C *per* day until a final temperature of 4°C was reached. Animals were housed at 4°C throughout the hibernation season, from November 2017 to April 2018. During this time, the light cycle was set to 22 h dark:2 h light to mimic burrow conditions while permitting daily monitoring, and animals were given food and water *ad libitum*.

2.2 Transmitter implantation

Body temperature radio telemeters (Models ETAF10 and TA-F10, Data Sciences International, St. Paul, MN) were implanted in 12 ground squirrels prior to the hibernation season to allow for real-time tracking of body temperature, which was used to determine whether squirrels were in torpor or IBE. Following an intra-peritoneal injection of slow-release buprenorphine, squirrels were anesthetized with 4% isoflurane gas. After the abdomen was shaved, an incision (of approximately 1 cm) was made along the mid-line of the abdomen, followed by an incision along the mid-line of the abdominal wall to expose the abdominal cavity. The transmitters were inserted in the abdominal cavity and the abdominal wall and skin were sutured using absorbable suture (Johnson&Johnson 4-0

coated VICRYL Plus 27” VCP310). Sterile saline (2 ml) was administered subcutaneously prior to placing the animals in a recovery chamber to prevent post-operative dehydration.

2.3 Tissue sampling protocol

Squirrels were euthanized in three experimental states: 1) summer-active (SA, n=8) where euthermic animals were sampled in late July 2017; 2) torpor (T, n=6), defined as a stable body temperature of ~5°C for 4 days, occurring from January through March 2018; and 3) inter-bout euthermia (IBE, n=6), defined as a stable body temperature of ~37°C for 4-5 h following a spontaneous arousal, also occurring from January through March 2018. Both SA and IBE squirrels were euthanized by lethal peritoneal injection of Euthanyl (0.7 ml of 240 mg/ml; Bimeda-MTC, Cambridge ON) followed by cervical dislocation, however, torpid squirrels were euthanized only by cervical dislocation to ensure an arousal was not induced by Euthanyl injection. Euthanyl does not influence mitochondrial metabolism (81).

2.4 Mitochondrial isolation

Mitochondria were isolated by differential centrifugation at 4°C and purified using a Percoll gradient, following established protocols (3, 63). Liver mitochondria were used in this study because significant metabolic suppression occurs in liver mitochondria between torpor and IBE (53), and the tissue has previously been demonstrated to tolerate I/R (49).

Following euthanasia, the liver was removed and minced in 1% BSA homogenization buffer (HB; 250 mM sucrose, 10 mM HEPES, 1 mM EGTA, pH 7.4). The minced tissue was transferred to a glass mortar and gently homogenized (three passes at 100 rpm) with a pre-chilled Teflon pestle. The homogenate was then filtered through one layer of cheesecloth into two centrifuge tubes and centrifuged at 4°C and 1,000 *g* for 10 mins. The supernatant was removed from each tube, filtered through four layers of cheesecloth into two clean pre-chilled 50 ml polycarbonate centrifuge tubes, and the centrifugation protocol was repeated. Again, the supernatant was removed and the

homogenate filtered through four layers of cheesecloth into clean tubes which were centrifuged at 8,700 g for 10 mins at 4°C to obtain a crude mitochondrial pellet. The extra-mitochondrial supernatant was discarded, and the remaining mitochondrial pellet was re-suspended in 500 µl BSA-free HB. The crude mitochondrial sample was carefully layered on top of a centrifuge tube containing a Percoll (Sigma-Aldrich) gradient solution which consisted of four 10 ml layers of Percoll diluted with BSA-free HB to different densities (10, 18, 30, 70% v/v). The Percoll gradient (and crude mitochondrial sample) was then centrifuged at 35,000 *g* for 35 mins at 4°C to obtain purified mitochondria, which settle between the 30% and 70% Percoll layers. The tube containing this purified sample was filled with BSA-free HB and centrifuged twice more at 4°C and 8,700 *g* for 10 mins to remove all Percoll, and the extra-mitochondrial supernatant was replaced with fresh BSA-free HB between spins. The final mitochondrial pellet was re-suspended in 1 ml BSA-free HB and aliquoted in pre-chilled Eppendorf tubes. One aliquot was kept on ice for respiration experiments, and the rest were flash-frozen in liquid N_2 and stored at -80°C for enzyme and Bradford protein assays (see sections 2.6 and 2.7).

2.5 *In vitro* performance metrics

2.5.1 Respirometry

The respirometry protocol was similar to an anoxia-reoxygenation protocol used for isolated turtle heart mitochondria (29), and one used for rat liver mitochondria (26) with the exception of how anoxia was established in the respirometer. Respiration rates of liver mitochondria were measured using Clark-type polarographic oxygen electrodes (Oxygraph-2k; Oroboros, Innsbruck AT). Mitochondria were suspended in 2 ml respiration buffer (MiR05: 110 mM sucrose, 60 mM K-lactobionate, 20 mM HEPES, 20 mM taurine, 10 mM KH_2PO_4, 3 mM $MgCl_2$, 0.5 mM EGTA, 1% (w/v) fatty-acid free BSA, pH 7.1) at a constant temperature of 37°C, and with constant stirring at 750 rpm. The Oxygraph-2k was calibrated both with air-saturated buffer and oxygen-depleted buffer (established using live yeast) before starting all experiments. Mitochondria (10-20 µl; 100-250 µg) were added to both chambers and a stable background respiration rate was established prior to the addition of any substrates. Respiration rates were determined using saturating concentrations of both NADH-linked (1 mM pyruvate, 1 mM malate)

and $FADH_2$-linked (6 mM succinate) substrates to ensure electron flux through complexes I and II. State 2 respiration rates (saturating substrate without ADP) were determined following the addition of substrates. State 3 (maximal, coupled respiration) rates were determined by titrating 0.1 mM ADP until a steady-state was observed, and state 4 (leak respiration) rates were established after depletion of the ADP by the mitochondria. Once state 4 was established, the chambers were opened slightly and nitrogen (N_2) gas was injected into the gas-space above the respiration buffer until the oxygen concentration decreased to ~5% of air saturation. At this point, the chambers were closed again and mitochondrial respiration drove the oxygen concentration of the chamber down to zero. Anoxia was maintained for five minutes, a duration which significantly alters the function of rat liver mitochondria *in vitro* (26, 30). The chambers were opened and re-oxygenated to 100% air saturation five min after anoxia was established. State 3 and state 4 respiration rates were determined again following this re-oxygenation. In preliminary experiments, oxidative substrates were added to the chamber following anoxia to ensure mitochondrial respiration rates were not limited by substrate availability. An example respirometry experiment is depicted in Figure 2-1A. Following these measurements, the content of the chambers was removed and centrifuged at 10,000 *g* for 10 mins at 4°C to obtain a mitochondrial pellet, which was frozen in liquid N_2 and stored at -80°C for enzyme assays.

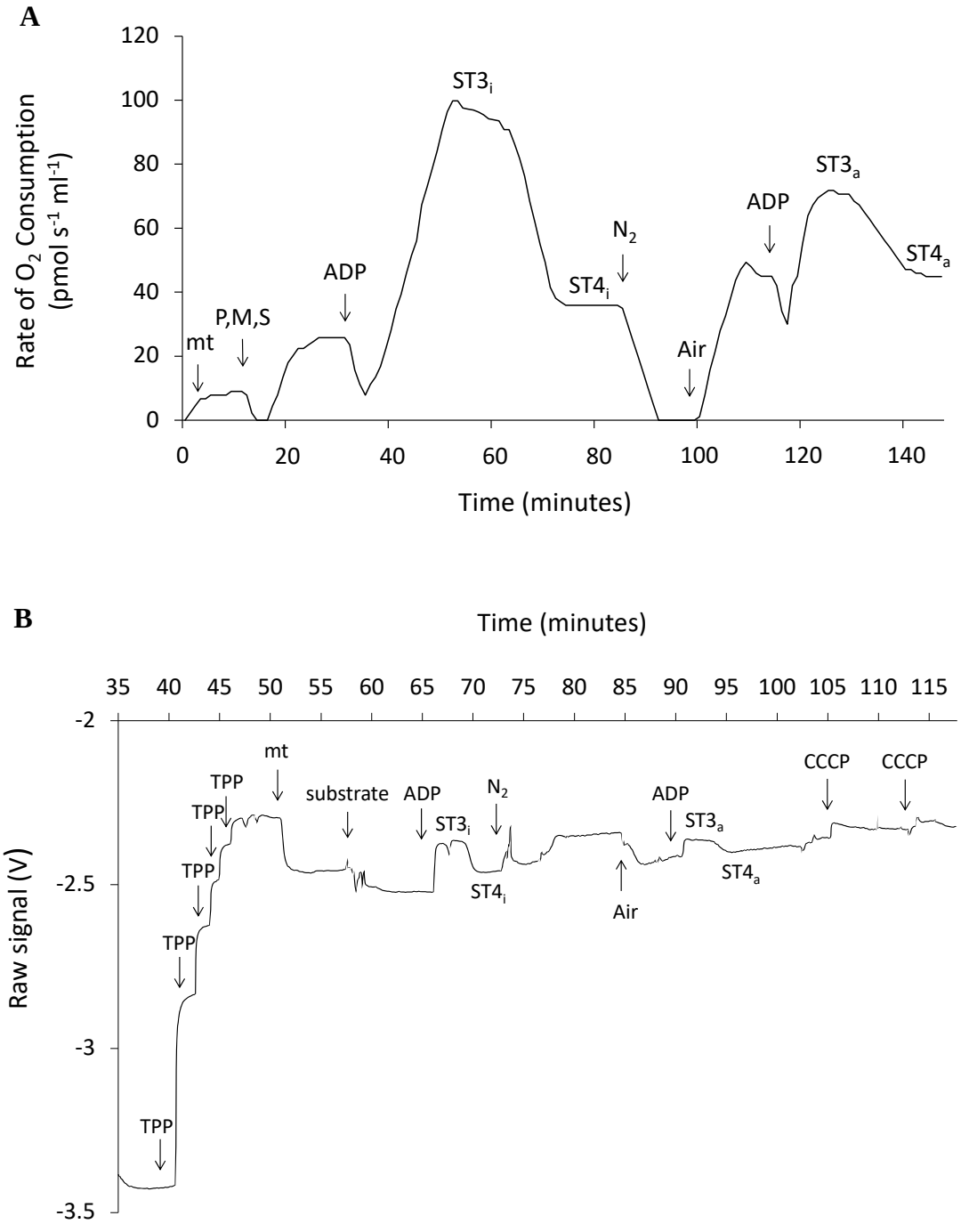

Figure 2-1. Representative traces for respiration rate (A) and membrane potential (B) determination. A decrease in electrode signal in (B) corresponds with membrane hyperpolarization. Mt=mitochondria, P,M,S=pyruvate, malate, succinate, $ST3_i$=initial state 3 rate, $ST3_a$=state 3 post-anoxia, $ST4_i$=initial state 4 rate, $ST4_a$=state 4 post-anoxia, TPP=tetraphenylphosphonium

2.5.2 Membrane potential

Mitochondrial membrane potential ($\Delta\psi_m$) was determined using a tetraphenylphosphonium (TPP^+) ion selective electrode (ISE; Oroboros, Innsbruck AT) and a Ag-AgCl reference electrode (MI-401; Microelectrodes Inc., Bedford NH). TPP^+ is a lipophilic ion that moves across phospholipid bilayers in proportion to $\Delta\psi_m$, and the electrodes measure extramitochondrial TPP^+. Electrodes were used in combination with the Oroboros-2k, in the same buffer used for respiration rate determination. Before mitochondria were added to the chamber, the TPP^+ electrode was calibrated by titrating with 4 µl injections (1 µM final concentration) of calibration solution (500 µM TPPCl, 100 mM KCl) step-wise until a final concentration of 5 µM TPPCl was reached inside the chamber. Once the calibration was complete, mitochondria were added to the chamber, and the same protocol was followed as with respiration experiments stated in Section 2.5.1 (ST3 and ST4 measurements before and after anoxia) with an anoxic exposure time of 5 mins. At the end of each experiment, 0.5 µM of a protonophore, carbonyl cyanide 3-chlorophenylhydrazine (CCCP), was titrated into each chamber to completely depolarize mitochondria in order to assess any drift in electrode function over time (see Figure 2-1B for an example of experimental workflow). Membrane potential was derived from the raw TPP^+ signal (extra-mitochondrial $[TPP^+]$) using a modified Nernst equation as described in (57):

$$\Delta\varphi_m = a \log \frac{([TPP^+]_{added} - [TPP^+]_{external})(0.16)}{(0.001)(mg\ protein)([TPP^+]_{external})}$$

Equation 1. Nernst equation for mitochondrial membrane potential ($\Delta\varphi_m$) determination. Where a = 2.3(RT/F) (R = the universal gas constant, T = absolute temperature in Kelvin, F = Faraday constant), 0.16 is a correction factor for how much TPP^+ binds non-specifically and does not cross the mitochondrial membrane (14), and 0.001 represents the liver mitochondrial volume of rats (34), which is assumed to be similar in ground squirrels (33). The $[TPP^+]$ added is the final $[TPP^+]$ in the respiratory medium after calibration (5 µM), and $[TPP^+]$ external is a measurement of extra-mitochondrial TPP^+ at a specific time-point.

2.6 ETS assays

Maximal activity of three electron transport system enzyme complexes (complex I, II, and V) was determined spectrophotometrically using original mitochondrial samples and samples recovered from the respiration experiments described in section 2.5 (above). Both samples were frozen in liquid N_2 and stored at -80°C prior to performing assays. These assays were performed using protocols outlined in (44). Mitochondrial pellets were resuspended in hypotonic medium (25 mM K_2HPO_4, 5 mM $MgCl_2$, pH 7.4) with phosphatase inhibitors (10 mM sodium fluoride and 1 mM sodium orthovanadate) and protease inhibitors (1x Protease Inhibitor Cocktail; ThermoFisher Scientific, Waltham MA) to a final concentration of 1 μg/μL prior to undergoing three freeze-thaw cycles in liquid nitrogen. Absorbance values (340 nm for complex I/V, 600 nm for complex II) were acquired using a SpectraMax plate spectrophotometer (Molecular Devices, Toronto ON) at 37°C and collected for 3-5 mins for each assay. Assays were run in triplicate for each sample. V_{max} values were calculated as the mean of these triplicates and corrected for pathlength and the extinction coefficient of each complex. For complex I activity determination, 5 μl of mitochondrial homogenate was added to 295μl of assay mixture (25 mM K_2HPO_4; pH 7.4, 2 μg/ml antimycin A, 2 mM KCN, 2.5 mg/ml BSA, 0.2 mM NADH). Complex II activity was measured following the addition of 1 μl of mitochondrial homogenate to 298 μl of assay mixture (25 mM K_2HPO_4; pH 7.4, 2 μg/ml rotenone, 2 μg/ml antimycin A, 2 mM KCN, 20 mM succinate, 50 μM dichlorophenolindophenol (DCPIP). The reaction was started with 1 μl of 10 μM ubiquinone$_1$. Complex V activity was measured following the addition of 5 μl of mitochondrial homogenate to 295 μl assay mixture (5 mM ATP, 1 mM phosphoenolpyruvate, 0.2 mM NADH, 1 U/ml pyruvate kinase, 1 U/ml lactate dehydrogenase).

2.7 Immunoblots

Prior to immunoblotting, the protein content of liver mitochondrial samples was determined using a Bradford assay. Mitochondrial samples (8.5 mg protein/ml) were denatured in sample buffer (4x Laemmli Sample Buffer) at 90°C for 5 min prior to

loading in 8-16% polyacrylamide Criterion TGX Stain-Free Gels (Bio-Rad, Mississauga, ON). Preliminary immunoblots were performed to identify the appropriate amount of protein to load into each well. Gels were loaded with 7.5 μg protein (for MnSOD) and 25 μg protein (for glutathione peroxidase-4) sample in each well and separated by electrophoresis at 120 V for 1 h in Tris-glycine-SDS running buffer (25 mM Tris, 192 mM glycine, 0.1% SDS). Following electrophoresis, gels were placed on a ChemiDoc imaging system (Universal Hood II, Bio-Rad, Mississauga, ON) for trans-illumination to ensure adequate protein cross-linking, which allowed for total protein fluorescence visualization using UV light. Total resolved protein content per lane, based on fluorescent intensity, was quantified using the densitometry analysis tool in ImageLab 5.2 (Bio-Rad). Proteins were then transferred to polyvinylidene fluoride (PVDF) membranes (Bio-Rad, Mississauga, ON) at 12 V and 4°C for 22 h. Membranes were blocked at 4°C for 16 h with 5% BSA in Tris-buffered saline (TBS-T; 20 mM Tris, 143 mM NaCl, 0.05% Tween-20) under constant agitation at 60 rpm. After blocking, membranes were probed with either MnSOD primary antibody (1:5000 in 2.5% BSA in TBS-T; Abcam, ab13533) or glutathione peroxidase 4 primary antibody (1:2000 in 2.5% BSA in TBS-T; Abcam, ab185689) with constant agitation at room temperature for 1 h. The membranes were briefly rinsed three times with TBS-T before washing with TBS-T under constant agitation for 15 min. Then, the TBS-T was replaced every five mins for three consecutive washes for a total of 30 minutes of washing. Following washes, the secondary antibody (Goat anti-rabbit, 1:10,000 in 2% BSA in TBS-T; Abcam, ab205718) was incubated with the membrane under constant agitation at room temperature for 1 h. Afterwards, membranes were washed (following the same protocol above) with TBS-T prior to imaging. Membranes were imaged using the ChemiDoc system and bands were visualized with Luminata Classico Western HRP Substrate (Millipore). Bands were quantified using the densitometry analysis tool in ImageLab 5.2 (Bio-Rad) and standardized to total protein loaded in each lane, determined using the UV visualization protocol.

2.8 Statistical analysis

Statistical analysis was performed using SPSS for ANCOVA and evaluation of estimated marginal means (EMM; the model is used to describe the effect of the dependent variable taking covariates into account, estimated at an x-value common to all three groups), and Prism 7.0 for one-way ANOVAs and paired t-tests when the F-statistic for ANCOVA models was not significant ($P>0.05$). The F-statistic was used to determine how well the model fit the data set, and a p-value over 0.05 indicated that the covariate (initial condition) could not explain differential effects of anoxia. Post-hoc tests to determine between-group and within-group statistical differences were performed following Bonferroni corrections. Data are expressed as mean ± SE for interaction plots. In the ANCOVA models, no interaction terms were significant in preliminary analyses and were therefore removed from regression equations prior to final analysis. R studio (R package version 3.1-131) was used to create ANCOVA figures only.

CHAPTER 3

3 RESULTS

3.1 Mitochondrial performance metrics

3.1.1 Mitochondrial respiration

When assayed at 37°C and with complex I-linked (pyruvate) and complex II-linked (succinate) substrates, maximal ADP-stimulated respiration rates (State 3; ST3) decreased after anoxia for all groups (Figure 3-1A). There were significant differences in initial ST3 rates among groups (One-way ANOVA: $F_{2,17}$=8.564, P=0.003). Specifically, initial ST3 in torpor was significantly lower than IBE (P=0.023) and summer (P=0.002) but there was no significant difference between IBE and summer ST3 (P=0.671). There were no significant differences in initial ST4 rates among groups (One-way ANOVA: $F_{2,16}$=2.40, P=0.123). It is reasonable to assume that post-anoxia ST3 (or ST4) would depend on initial ST3 (or ST4), so I analyzed these data using an ANCOVA model (with initial ST3 or ST4 as a covariate) to control for initial group differences.

There was a significant effect of both initial ST3 (P<0.0001) and group (i.e. hibernation condition; P=0.029) on post-anoxic ST3 (ANCOVA: $F_{3,16}$=9.602, P=0.001; Figure 3-2). The relationship between initial and post-anoxia ST3 was virtually identical in SA and IBE, but in torpor ST3 was elevated. As a result, when compared at an initial ST3 value of 105.8 nmol O_2 ml^{-1} min^{-1} mg $protein^{-1}$, a value common to all groups selected by the ANCOVA model, the final ST3 of torpid liver mitochondria was significantly higher than IBE (P=0.033; as shown by EMM values in Figure 3-2) and at the margin of significance (P=0.054) compared to summer. A reduction in ST3 after anoxia indicates reduced ETS capacity, which could result from either reduced substrate oxidation or reduced ATP synthesis.

Leak respiration (State 4; ST4) increased approximately two-fold in summer liver mitochondria after anoxia (Figure 3-1B). These data were also analyzed using an ANCOVA, as ST4 post-anoxia was assumed to correspond with initial ST4. There was a significant effect of both initial ST4 (P<0.01) and group (P<0.01) on final ST4

(ANCOVA: $F_{3,14}$=9.308, P=0.001; Figure 3-3). When compared at a common initial ST4 value of 25.44 nmol O_2 ml^{-1} min^{-1} mg $protein^{-1}$, the final ST4 of summer liver mitochondria was significantly higher than IBE (P=0.003) and torpor (P=0.016). An increase in ST4 after anoxia may indicate higher proton conductance across the IMM. There was also a significant effect of anoxia on the respiratory control ratio (RCR) in all groups (Figure 3-4; torpor: t_5=7.02, P<0.001; IBE: t_4=2.78, P=0.0498; SA: t_6=6.91, P<0.001), however the RCR of torpid mitochondria decreased the least following anoxic exposure. In general, mitochondrial respiratory function is better maintained in torpor mitochondria than in either IBE or summer following anoxia.

3.1.2 Membrane potential

When assessed during ST4 respiration, initial mitochondrial membrane potential did not differ significantly among groups (One-way ANOVA: $F_{2,8}$=1.21, P=0.348). These data could not be effectively modeled using an ANCOVA as with ST3 and ST4 (ANCOVA: $F_{3,7}$=1.64, P=0.265), so I used paired t-tests to look at the effect of anoxia on membrane potential within each group. This revealed no overall effect of anoxia on membrane potential (Figure 3-5; torpor: t_4=1.53, P=0.2; IBE: t_2=1.85, P=0.2), however, there was a marginally significant depolarization of SA mitochondria after anoxia (t_2=4.18, P=0.053; Figure 3-5).

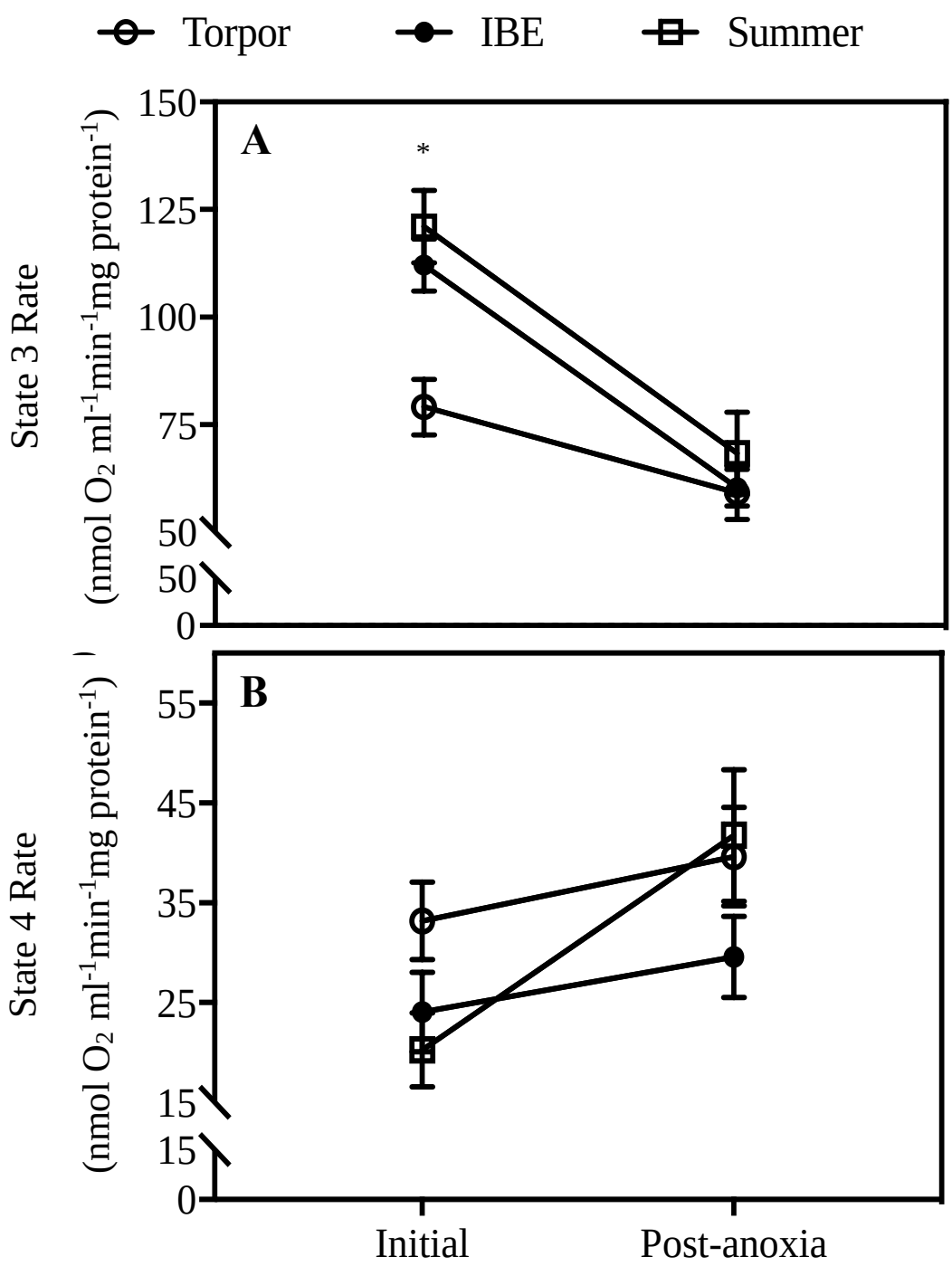

Figure 3-1. Interaction plots of complex I- and II-linked state 3 respiration (A) and state 4 respiration (B) of liver mitochondria before (initial) and after 5 minutes of anoxia. Data presented are mean ± SE. This plot demonstrates the general effect of anoxia on mitochondrial respiratory performance. There is a significant difference between torpor and both IBE and summer for initial ST3 (*, $P \leq 0.05$, Panel A). Further statistical analyses of these data are presented in Figures 3-2 and 3-3.

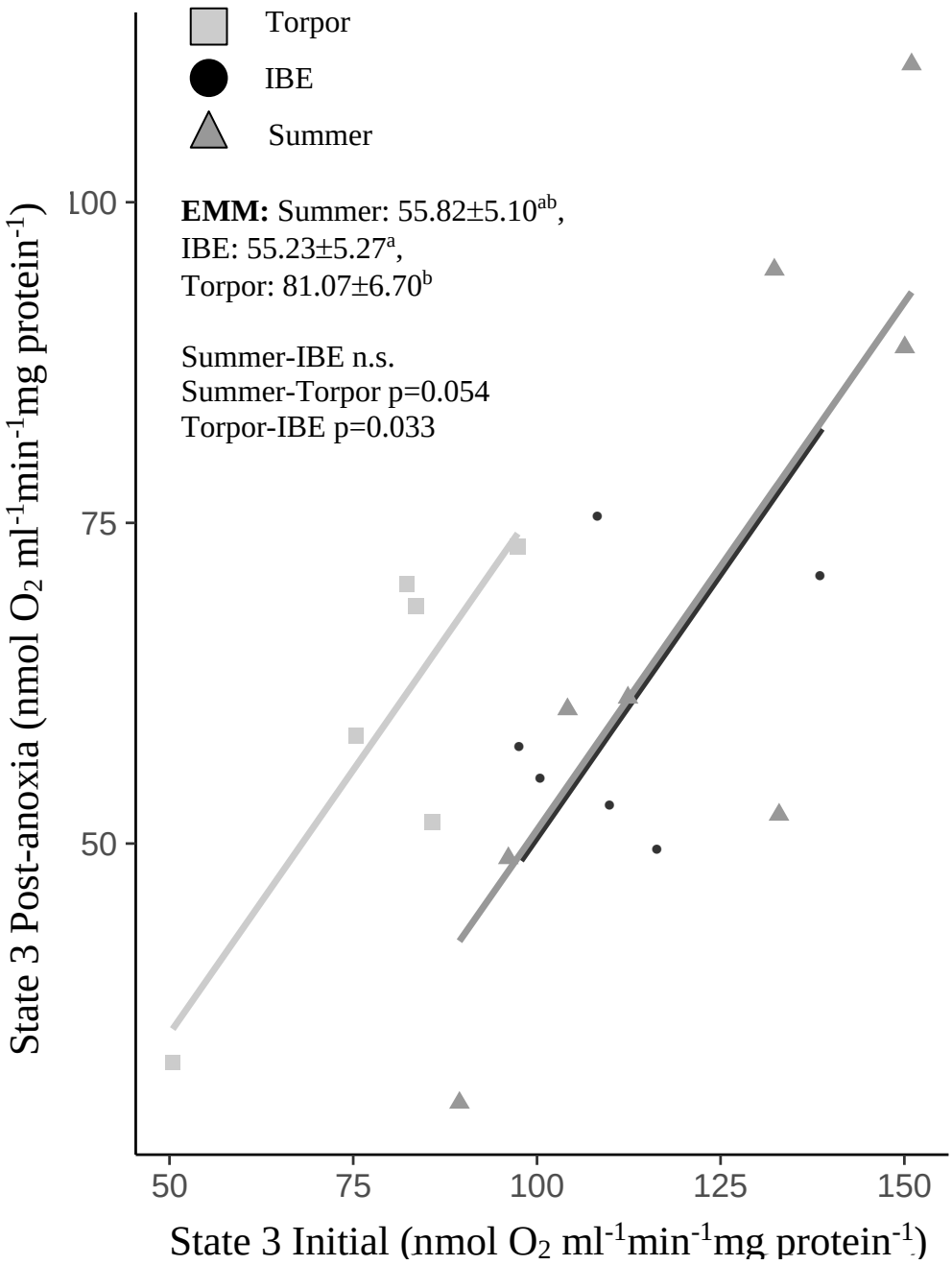

Figure 3-2. Post-anoxia state 3 respiration rates of liver mitochondria as a function of initial state 3 rates. ANCOVA revealed a significant effect of both initial ST3 ($P<0.0001$) and group ($p=0.029$) on post-anoxia ST3. Estimated marginal means (EMM) were evaluated at an initial ST3 value of 105.79 nmol O_2 $ml^{-1}min^{-1}mg$ $protein^{-1}$. This analysis revealed a significantly greater effect of anoxia on ST3 in IBE compared with torpor. Significant differences among groups (assessed using EMMs) are presented in the figure legend for torpor (N=6) IBE (N=6) and summer (N=8), where differential lettering beside EMM values represents statistical significance between groups ($P \leq 0.05$).

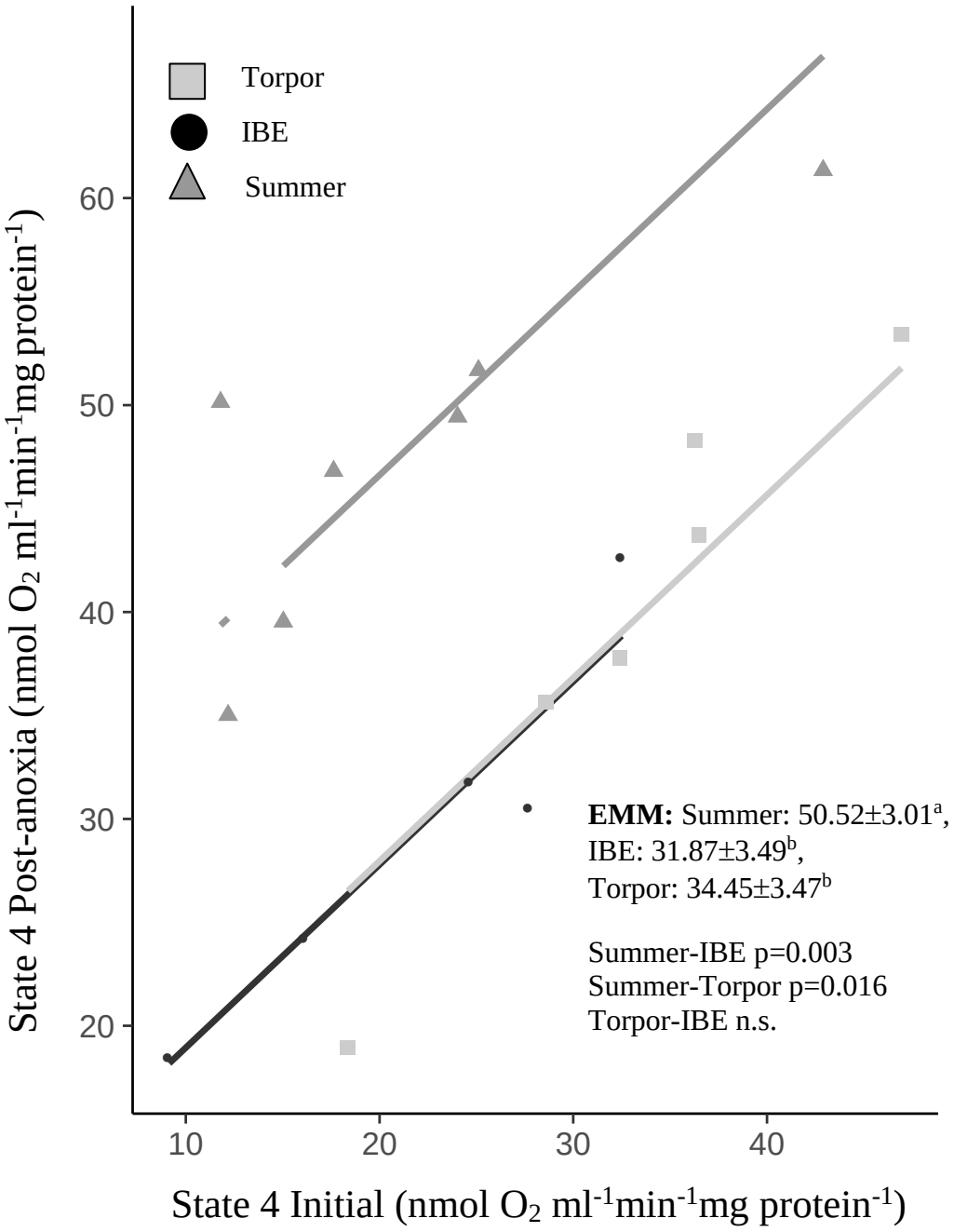

Figure 3-3. Post-anoxia state 4 respiration rates of liver mitochondria as a function of initial state 4 rates. ANCOVA revealed significant effects of both initial ST4 ($P<0.01$) and group ($P<0.01$) on post-anoxia ST4. Estimated marginal means (EMM) were evaluated at an initial ST4 value of 25.44 nmol O_2 $ml^{-1}min^{-1}mg$ $protein^{-1}$. This analysis revealed that anoxia had a significantly greater effect on ST4 in summer than in either torpor or IBE. Significant differences among groups (assessed using EMMs) are presented in the figure legend for torpor (N=6) IBE (N=5) and summer (N=7), where differential lettering beside EMM values represents statistical significance between groups ($P\leq0.05$).

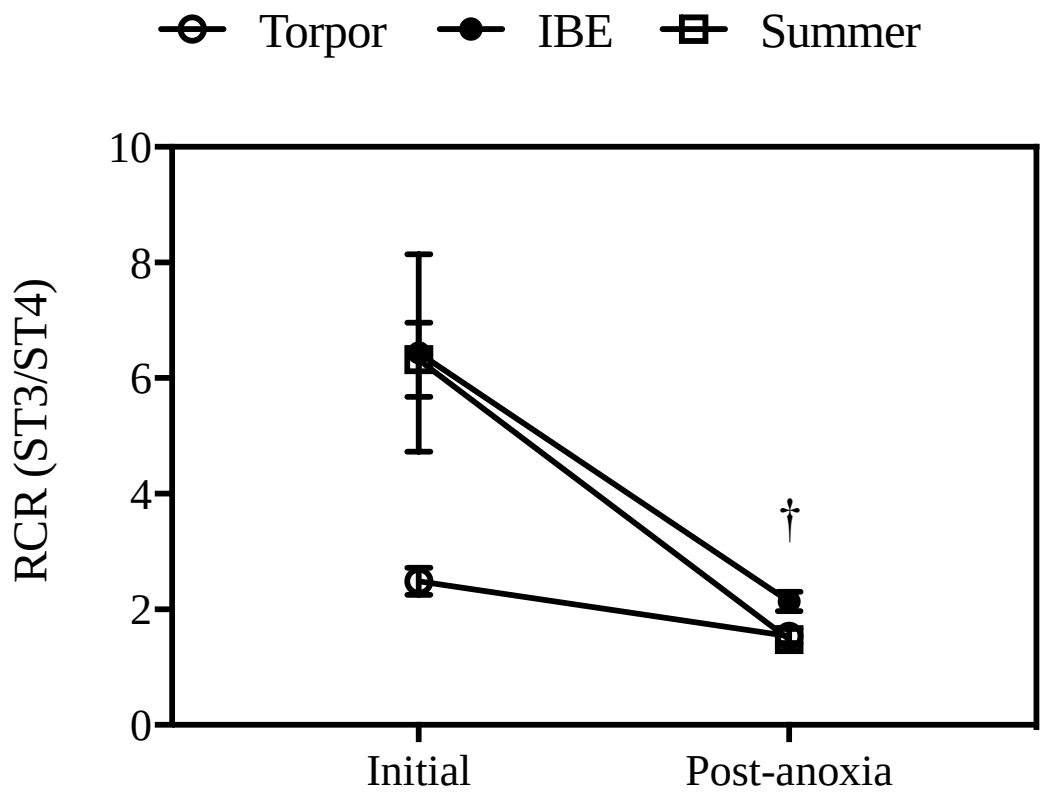

Figure 3-4. Interaction plot of the respiratory control ratio (RCR) of liver mitochondria before (initial) and after 5 minutes of anoxia. Data are presented as mean ± SE for N=6 torpor, N=5 IBE and N=7 summer mitochondrial samples, analyzed using paired t-tests for each group. Anoxia significantly decreased RCR in all groups (†, $P<0.001$ for both torpor and SA and $P=0.05$ for IBE).

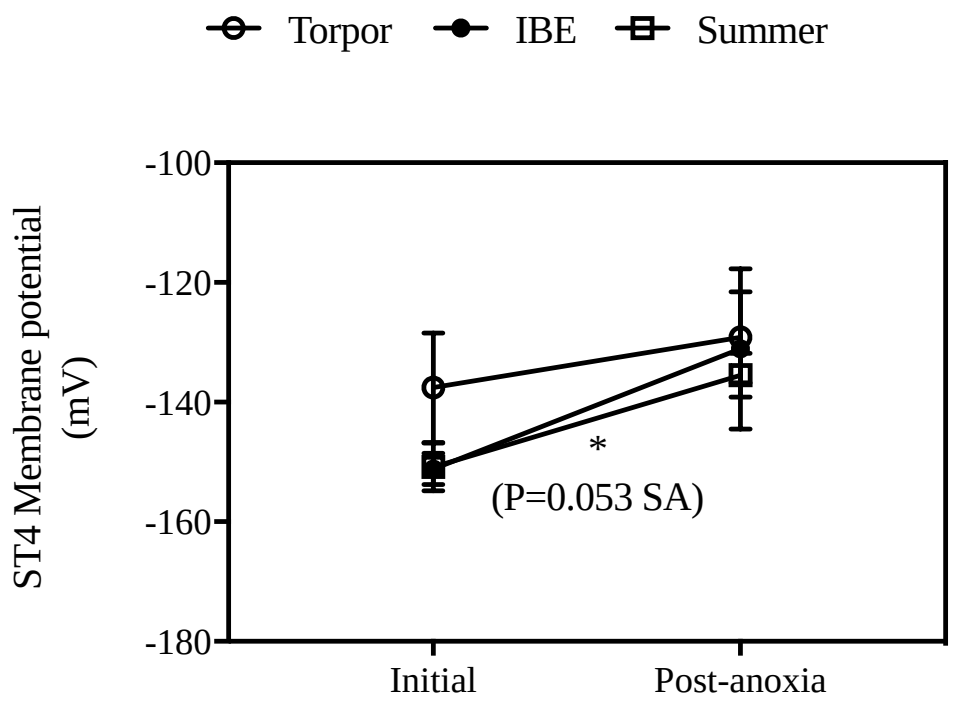

Figure 3-5. Interaction plot of membrane potential of liver mitochondria before (initial) and after 5 minutes of anoxia, measured during state 4 respiration. Data presented are mean ± SE for N=5 torpor, N=3 IBE, and N=3 summer. These data were analyzed using paired t-tests for each group. Overall, there were no significant within-group differences in this effect. However, the effect of anoxia on ST4 membrane potential in summer squirrels was at the margin of significance (*, P=0.053).

3.2 Mitochondrial complex assays

Enzyme complex assays were performed on mitochondrial samples frozen immediately after isolation or recovered from respirometry trials following anoxia exposure to determine whether changes in mitochondrial performance were reflected by changes to electron transport system (ETS) capacity. Post-anoxia enzyme activity could not be appropriately modeled using an ANCOVA model because the F-statistic failed to reach significance in all three models (Complex I $F_{3,11}$=0.617, P=0.618; Complex II $F_{3,11}$=3.24, P=0.064; Complex V $F_{3,11}$=0.649, P=0.560). Paired t-tests determined that complex II activity of IBE mitochondria decreased after anoxia (t_4=3.24, P=0.032; Figure 3-6) as did complex I activity of summer mitochondria (t_3=9.51, P=0.002; Figure 3-6). However, there was no effect of anoxia on complex V activity in any group, and torpid mitochondria were not affected by anoxia in terms of complex I, II, or V activity (Complex I: t_5=1.45, P=0.2; Complex II: t_5=0.72, P=0.51; Complex V t_5=1.14, P=0.31). Thus, anoxia decreased maximal ETS enzyme capacity in IBE (complex II) and summer mitochondria (complex I), but no changes occurred with anoxia in torpor mitochondria.

3.3 Constitutive antioxidant enzyme expression

Western blots were used to quantify constitutive antioxidant expression in SA, IBE, and torpor mitochondria. There was no significant difference in mitochondrial MnSOD content among groups (One-way ANOVA: $F_{2,9}$=0.563, P=0.588; Figure 3-7). GPx4 content was significantly different among groups (One-way ANOVA: $F_{2,9}$=5.805, P=0.024). IBE mitochondria had higher expression of GPx4 compared to summer (t_9=3.061, P=0.0407) and expression was at the margin of significance compared to torpor (t_9=2.827, P=0.0595).

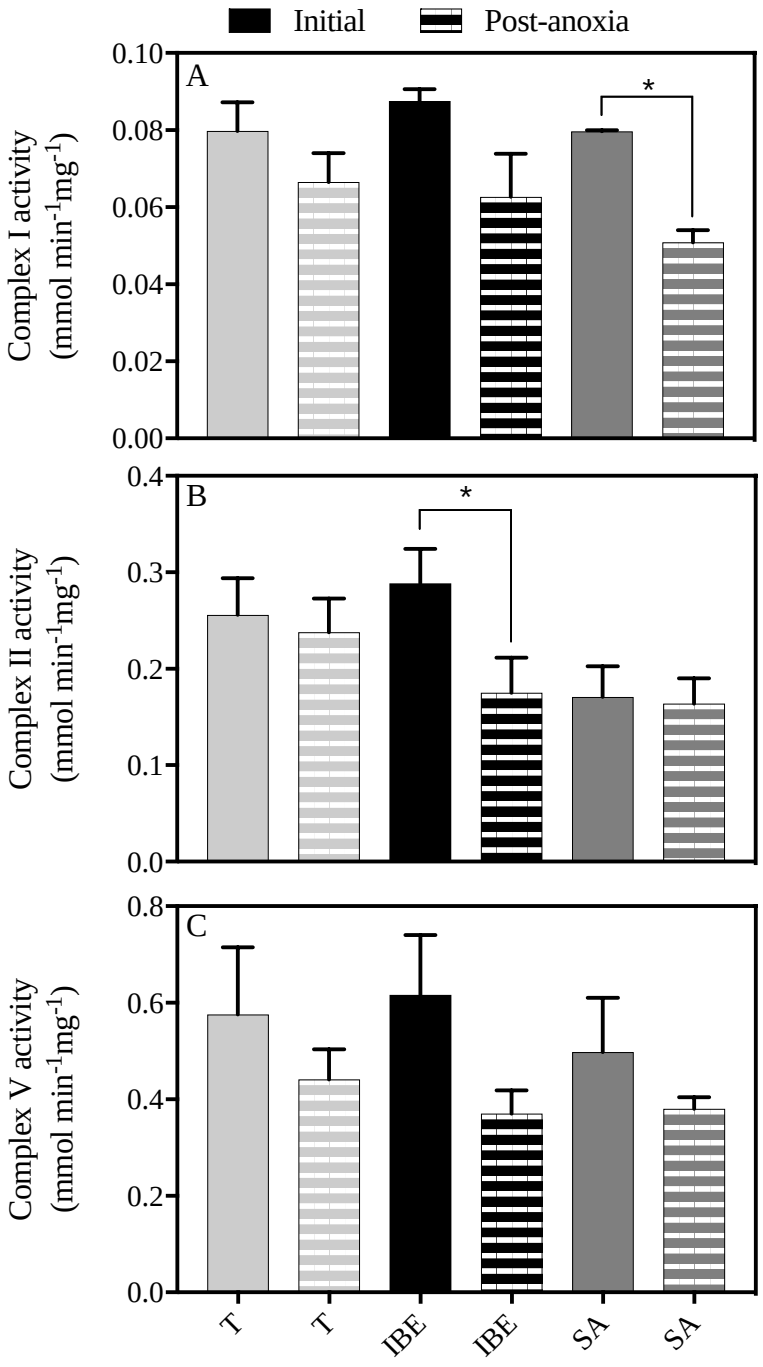

Figure 3-6. Maximal activity of ETS Complex I (A) Complex II (B) and Complex V (C) from liver mitochondria before (initial) and after anoxic exposure. Data are presented as mean ± SE for both the original mitochondrial sample, and the sample recovered from the Oxygraph following respiration measurements for N=6 torpor N=5 IBE and N=5 summer samples. These data were analyzed using paired t-tests within each group. Anoxia significantly decreased complex I activity in summer (*, P=0.0025; Panel A) and complex II activity in IBE (*, P=0.0316; Panel B) but had no significant effect in torpor.

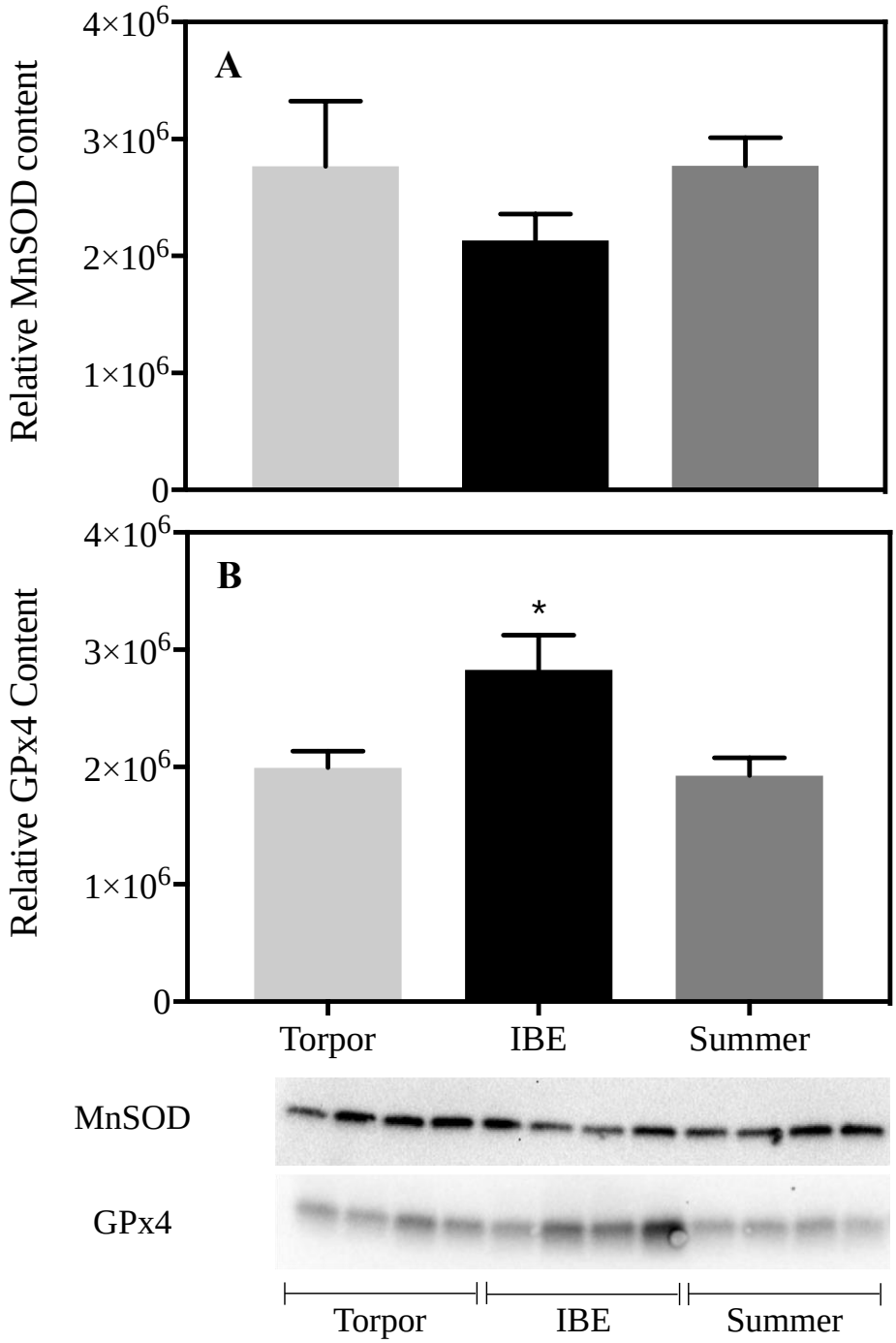

Figure 3-7. Relative MnSOD (A) and Glutathione Peroxidase-4 (GPx4; B) content of liver mitochondria. Data are presented as mean ± SE for N=4 torpor, IBE, and summer samples. Data (acquired by densitometry) are normalized to total protein loaded in each well. There were no significant differences among groups in terms of MnSOD content. GPx4 content is significantly higher in IBE than summer (*, P=0.0407) and at the margin of significance compared to torpor (P=0.0595).

CHAPTER 4

4 DISCUSSION

The aim of this study was to determine whether mitochondria isolated from ground squirrels during hibernation had enhanced anoxia tolerance compared to euthermic summer ground squirrels. There is substantial evidence that hibernating animals avoid tissue damage that is typically associated with hypoxia-reoxygenation (25, 46, 49). Moreover, this protective phenotype at the tissue-level is shared by both torpid and euthermic animals during the hibernation season, so it is likely not a direct consequence of low temperature or metabolic suppression, at least at the level of the tissue. Tolerance to hypoxia may be attributed to oxidative stress avoidance, or an enhanced capacity to avoid apoptosis following oxidative stress, which could be affected by metabolic state. I hypothesized that metabolic flexibility during hibernation would permit anoxia tolerance at the mitochondrial level, and would correspond with previous research conducted at the tissue level.

4.1 The effect of anoxia on mitochondrial performance

Maximal ADP-stimulated respiration rates of liver mitochondria were consistent with previous literature on other hibernators (reviewed in 77), including 13-lined ground squirrels (53), however the degree of metabolic suppression in torpor was lower in my experiment (30% suppression) than in previous studies (60% suppression using succinate as substrate; 53). This apparent discrepancy is likely because I used both complex I- and complex II-linked substrates, whereas previous studies used complex II-linked substrate only, which demonstrated the greatest degree of suppression between torpor and IBE. I report ST4 respiration rates that are approximately 3-fold higher in torpor than rates reported previously for torpid thirteen-lined ground squirrels (22). Again this difference is likely due to my use of both pyruvate and succinate, compared with earlier studies that used only succinate as substrate and inhibited complex I using rotenone. In this study, complex I was not inhibited and its proton pumping could contribute to a higher protonmotive force (Δp). At higher (Δp), ST4 respiration would be expected to increase, similar to the effect seen in rat liver mitochondria (12). This higher Δp would accelerate

proton leak across the IMM (9), thereby increasing ST4 respiration rates. Chung *et. al.* (ref. 22) also report ST3 rates much lower than in this study (60% lower for both IBE and torpor), which could reflect a lower Δp.

In support of my hypothesis, liver mitochondria from torpid ground squirrels maintained oxidative phosphorylation performance better after anoxia than IBE or summer mitochondria. Anoxia decreased ST3 respiration rate in all groups, but torpor was affected the least, falling by 25% of initial values, compared with 43% for SA and 46% for IBE (Figures 3-1A and 3-2). Leak (ST4) respiration rates increased by 135% after anoxia in summer mitochondria, but not in IBE or torpor (Figures 3-1B and 3-3). Not surprisingly, the RCR (ST3/ST4) of torpor mitochondria was least affected by anoxia (Figure 3-4), likely owing to the marginal decrease in ST3 and maintenance of ST4. Taken together these results suggest that mitochondria isolated from torpid ground squirrels maintain bioenergetic integrity better than those from summer and IBE animals. The effect of anoxia on summer ground squirrel mitochondria is consistent with current literature on the effect of *in vitro* anoxia-reoxygenation on rat mitochondrial bioenergetics. One minute of anoxia with subsequent re-oxygenation increases ST4, and decreases ST3, RCR, and oxidative phosphorylation efficiency (P/O ratio) in isolated liver mitochondria (26) and heart mitochondria (4) in rats.

Differential tolerance to anoxia-reoxygenation (A/R) in this study is likely related to ROS production, as different durations of anoxia did not differentially affect mitochondrial performance (see Appendix 3). ROS scavenging capacity may play a role in differential tolerance to A/R because GPx4 content was significantly elevated in IBE and was at the margin of significance in torpor compared to SA squirrels. However, MnSOD content does not differ among groups (Figure 3-7). Future analysis of antioxidant activity and expression of different antioxidants (such as vitamin E, GSH, thioredoxin-2, and peroxiredoxins) is warranted. Additionally, tolerance to A/R is likely not exclusively an effect of lower mitochondrial metabolic rate in torpor. Rat liver mitochondria showed a significant decrease in mitochondrial performance after A/R despite initial ST3 and ST4 rates lower than torpid ground squirrels (see Appendix 2).

4.1.1 Membrane potential ($\Delta\psi_m$) and ST4 respiration

Anoxia had a significant overall depolarizing effect on membrane potential, however, the effect was subtle such that during ST4, membrane potential did not increase significantly within any of the groups. This mild depolarization corresponded with an increase in ST4 respiration following anoxia, which suggests an increase in proton conductance across the IMM. An increase in proton conductance would necessitate increased ST4 respiration to maintain Δp (13, 54). Therefore, greater increases in ST4 after anoxia in SA mitochondria (with no change in $\Delta\psi_m$) likely indicates greater proton conductance of the IMM. This effect may result from activation of proteins that increase proton conductance or from damage to IMM components in response to A/R.

Superoxide and hydroxynonenal (HNE; a product of lipid peroxidation) can increase proton conductance across the IMM mediated by uncoupling proteins (UCPs) and the adenine nucleotide translocase (ANT) (43). Mild uncoupling of substrate oxidation from ATP synthesis can regulate ROS; high Δp increases the lifetime of reduced electron carriers in the ETS which promotes ROS production (54) so even mild uncoupling may decrease ROS production. Some superoxide production is expected upon re-oxygenation from complete anoxia, so activation of the ANT or UCPs are mechanisms that may explain the depolarizing effect of anoxia, especially in mitochondria from SA ground squirrels. Other than UCP and/or ANT activation, A/R could cause ROS-induced peroxidation of IMM phospholipids and subsequent increases in permeability and therefore proton conductance (2, 83, 91). As a result, increased electron flux through the ETS would be required to maintain Δp (13, 54). Such increases in ST4 have also been attributed to opening of the permeability transition pore (PT pore; ref. 56) which is discussed more below.

To assess whether uncoupling is mediated by UCPs or ANT, one can use their specific inhibitors, GDP and carboxyattractyloside (CAT). Mitochondria isolated from rat hearts subjected to I/R show increases in ST4 (relative to pre-I/R values), which are inhibited ~60% by CAT, and only minorly inhibited by GDP (56). Apart from UCP- and ANT-mediated uncoupling, the opening of the PT pore was responsible for increases in

ST4 in heart mitochondria (56), which is a pathological consequence of I/R that can lead to apoptosis or necrosis (35). Mitochondria isolated from rat hearts preconditioned to brief I/R showed only minor increases in ST4 after I/R, and this effect was completely inhibited by GDP and CAT. Any treatments that prevented increases in ST4 after I/R were associated with improved recovery from I/R (56).

ST4 respiration typically accounts for 20-40% of basal respiration in hepatocytes (11). After anoxia, ST4 respiration increased by 135% in summer mitochondria, compared to 23.3% in IBE and 19.2% in torpor. These results suggest that, although the degree of depolarization following anoxia did not differ among groups, SA mitochondria had to consume more O_2 to maintain the newly established $\Delta\psi_m$. Typically, as mitochondrial $\Delta\psi_m$ increases, O_2 consumption increases exponentially—the so-called "non-ohmic" relationship (43)—at least under normoxic conditions. So, a lower $\Delta\psi_m$ would be expected to disproportionately decrease the substrate oxidation and O_2 consumption required to offset proton leak. In contrast to this typical relationship between ST4 and $\Delta\psi_m$, ST4 increased in all groups following A/R despite modest decreases in $\Delta\psi_m$, but the increase in ST4 was greatest in SA mitochondria.

Thus, the greater increase in ST4 in SA mitochondria may indicate a greater ROS-mediated response to A/R than in either torpor or IBE. This response may correspond with differences in activation of proton conducting proteins (UCPs or ANT) or differential damage to the IMM among hibernation/seasonal states. Higher GPx4 content in IBE mitochondria (Fig 3-7) may protect against ROS-induced increases in ST4, as GPx4 plays a role in phospholipid peroxide metabolism and detoxification (23, 31, 42).

4.1.2 ST3 respiration

Reductions in ST3 respiration following ischemia and reperfusion are often paralleled by decreases in the function of electron transport system (ETS) components (19). During myocardial ischemia, loss of complex I function occurs early during an ischemic episode, while complex III and IV become progressively damaged if the ischemic insult persists longer than 30-45 minutes (19). Decreased complex I dysfunction after ischemia is associated with dissociation of the flavin mononucleotide (FMN; 70). This dysfunction is

likely ROS-related: molecules that block the ubiquinone binding site of complex I (I_Q; a known site of superoxide production, Brand 2016) also prevent decreases in complex I function after ischemia (19).

The significant decrease in ST3 that I observed in summer and IBE mitochondria may be attributable, in part, to ETS complex dysfunction. Anoxia decreased maximal activities of complex I (by 36%) and complex II (by 39%) in summer and IBE liver mitochondria, respectively (Figure 3-6), while these complexes were not affected by anoxia in torpor mitochondria. Lower ETS complex activity will constrain oxidative phosphorylation capacity, but ETS component damage can also lead to increased ROS production (19). ROS production can initiate a cascade of deleterious effects, including lipid peroxidation, which can increase membrane permeability (2, 83, 91). An increase in ST4 respiration occurred as a result of A/R in SA squirrels, which could indicate increased ROS production and membrane permeability.

Overall, mitochondria isolated from squirrels during torpor are least affected by *in vitro* A/R, while mitochondria isolated from SA squirrels are most affected. It is likely that ROS production or detoxification is involved in differential tolerance to A/R. High ROS production can affect mitochondrial performance through the following mechanisms: (i) activation of UCPs and ANTs which can increase ST4 and depolarize ψ_m; (ii) lipid peroxidation and increased membrane permeability which can increase ST4 and depolarize ψ_m; (iii) ETS complex damage which can decrease ST3 and further increase ROS production. A/R only marginally affected ST4 respiration in IBE and torpor, and ST3 was least affected in torpor mitochondria. A/R also had no effect on the maximal activity of complex I, or II in torpor, but did affect complex I in SA mitochondria and complex II in IBE mitochondria. These data suggest that during torpor (and IBE to a lesser extent) mitochondrial respiration is maintained primarily due to low electron leak following A/R.

4.2 Mitochondrial targets for ischemia-reperfusion tolerance

The mechanisms that appear to protect winter ground squirrel mitochondria from A/R may be analogous to known models that demonstrate protection from I/R injury.

Brief periods of ischemia and reperfusion can protect tissues against future ischemic events in a process called ischemic preconditioning (IPC). The mechanisms of IPC remain unclear, but there are several proposed triggers and effectors (reviewed in 92). More recent research has focused on the effect of IPC on complex I activity. Adenosine may mediate IPC, specifically through activation of NO synthesis. Administration of exogenous NO to perfused rat liver confers cytoprotection following ischemia and reperfusion (62). Also, *in vitro* nitrite administration during anoxia in isolated liver mitochondria preserves ST3 after anoxia better than the control (saline) treatment. Nitrite administration was associated with reduced ROS production, which could explain improved anoxia tolerance (74).

The mechanism of cytoprotection by NO likely involves protein S-nitrosylation (a post-translational modification that involves the attachment of NO to cysteine residues), which has been implicated in cardiac IPC (21, 80) perhaps because it specifically inhibits complex I as well as ATP synthase (21). Interestingly, the inhibitory effect of S-nitrosylation on complex I is oxygen-dependent, and is reversed after reperfusion; however, the reversal is slow and reduces ROS production during reperfusion as a result (21). These effects are similar to the protection offered from pharmacological inhibition of complex I. Prior to an ischemic event, pharmacological inhibition of complex I with amobarbital prevents decreases in ST3 in rat heart mitochondria after subsequent ischemia and reperfusion (20).

Although S-nitrosylation of complex I has not been identified in mitochondria from hibernators, ETS complex modifications exist between hibernation states. These modifications may affect ROS production perhaps explaining the differential tolerance to A/R shown in my study. The activity of complex I did not differ among groups in this study, but previous research conducted by our group has shown a decrease in complex I activity of liver mitochondria from torpor relative to IBE (53). The phosphorylation state of complex I differs between torpor and IBE, which could explain differences in maximal activity (52). Also, flux through complexes I-IV (assessed using complex I-linked substrates only) is significantly lower in torpor compared to IBE (52), suggesting differential activity of TCA cycle enzymes or lower rates of pyruvate oxidation. The

presence of these post-translational modifications (PTMs) may have similar advantages in A/R as S-nitrosylation or pharmacological inhibition of complex I. It is also likely that differential flux between torpor and IBE can involve PTMs that have not been investigated in liver mitochondria of hibernators. Identifying other PTMs that change during hibernation or seasonally could help elucidate mechanisms of anoxia tolerance, as some may mitigate oxidative stress.

4.3 Mechanisms of anoxia tolerance in hibernator mitochondria

4.3.1 Pre-hibernation test drops and ischemic preconditioning

Just prior to the hibernation season, many hibernators undergo brief bouts of metabolic suppression and T_b depression referred to as “test drops” that are similar to torpor-arousal cycles physiologically, but less extreme in terms of duration, and the degree of both metabolic rate and T_b depression (32, 73, 79). In the 13-lined ground squirrel, these test drops often occur before relocation into the hibernaculum for winter (at a T_a of 21°C), and last less than two days with T_b reaching a minimum of ~20°C (71). If evidence of transient hypoxia exists on arousal from torpor, a similar (less severe) hypoxic event could occur during test drops, which could have a preconditioning effect on certain tissues similar to IPC described in section 4.2 and reviewed in ref. 90.

Similar to S-nitrosylation, small ubiquitin-related modifiers (SUMOs; important PTMs) have been implicated in IPC (47). Covalent binding of SUMO to lysine residues on target proteins modifies their function (89). These PTMs are specifically upregulated during torpor in 13-lined ground squirrels in several organs (47). Increased SUMO conjugation (induced by IPC) in neuroblastoma cells offers cytoprotection from oxygen and glucose deprivation, which is analogous to ischemia-reperfusion (47), however the specific proteins modified by SUMOylation were not reported in this study.

Though it is unknown whether preparation for hibernation establishes a protective phenotype typical of IPC, cold exposure alone has been associated with mitochondrial stress resistance in ground squirrel neuronal stem cells (58). Exposure of induced pluripotent stem cells (iPSCs) to acute cold (4°C for 4 h) upregulated genes specific to

the mitochondria and protein quality control (heat shock proteins, proteases, and proteinase inhibitors) in ground squirrel iPSCs, but not human iPSCs. Phenotypically, cold-exposed ground squirrel iPSCs had a depolarized mitochondrial membrane potential relative to iPSCs maintained at 37°C, which was associated with low ROS production. By contrast, cold-exposure of human iPSCs increased both mitochondrial membrane potential and ROS production, an effect which was mitigated with a mild mitochondrial uncoupler (58). The T_a for the ground squirrels used in my study was set to 5°C for the entire hibernation season. It is plausible that the genes involved in protein quality control that were upregulated after cold exposure in ground squirrel iPSCs are also upregulated in torpor and IBE in my study, which could explain better maintenance of mitochondrial performance after A/R compared to SA squirrels. Additionally, although resting membrane potential did not differ among groups in my study, a decrease in ψ_m has been reported previously in Arctic ground squirrels during torpor (5), which could have similar effects on ROS production as seen in iPSCs. Future respirometry studies should be performed at 5°C to see whether the effects of cold exposure on ground squirrel iPSCs are also observed in liver mitochondria during torpor, which would better represent the environmental conditions in which transient hypoxia may occur upon early arousal.

4.3.2 Other potential mechanisms of anoxia tolerance in hibernators

In addition to SUMOylation, proteomic and metabolomic studies have reported different levels of proteins and small molecules both seasonally and during hibernation that may relate to stress tolerance. A study comparing the hepatic proteome of SA 13-lined ground squirrels and squirrels during entrance into torpor (Ent) found that proteins involved in anti-apoptosis, apoptosis regulation, and cellular redox status were specifically upregulated in Ent compared to SA (69). Additionally, a comprehensive study of plasma metabolites in 13-lined ground squirrels revealed an increase in plasma cysteine and cystathionine during late torpor (24), which are substrates for the cystathionine beta synthetase (CBS) enzyme that produces hydrogen sulfide (H_2S). H_2S is thought to be an important regulator of ROS production through its inhibition of complex IV in mitochondria, and administration of H_2S during reperfusion of ischemic mouse hearts was correlated with higher ST3 in isolated heart mitochondria compared to a

vehicle control (27). Since H_2S binds to complex IV with a low affinity, its inhibitory effect occurs predominantly during periods of low oxygen (68) and therefore is a plausible mechanism for mitochondrial A/R tolerance.

It is well established that ETS complexes can assemble into higher-order structures known as supercomplexes (1), and that these supercomplexes can increase respiration efficiency and reduce ROS production (60). Cardiolipin is a phospholipid that is known to stabilize supercomplexes (60, 64) and cardiolipin content of liver mitochondria increases by 50% in Arctic ground squirrels in the winter compared to the summer (45). Differential tolerance to A/R is best explained as a function ROS production in my study. If supercomplex stability is truly enhanced in hibernators during the winter compared to summer, this may contribute to reduced ROS production and therefore protection from A/R during hibernation.

There are various physiological changes that correspond with the seasonal transition to hibernation and the transition from torpor to IBE that may confer tolerance to A/R at the mitochondrial level. These data suggest that the IBE state confers some tolerance to A/R compared to SA, and this effect is enhanced in torpor. Differential ROS production and scavenging capacity may underlie these differences. I propose that the mechanisms conferring tolerance to A/R during hibernation may include: (i) PTMs that suppress activity of ETS enzymes and prevent ROS production in torpor; (ii) increased antioxidant capacity in IBE; (iii) upregulation of proteins associated with stress tolerance in IBE and torpor; and (iv) enhanced supercomplex stability and lower ROS production in IBE and torpor. Functional analyses should investigate these specific pathways to elucidate their role in hypoxia tolerance.

CHAPTER 5

5 CONCLUSIONS AND FUTURE DIRECTIONS

The goal of this study was to determine whether mitochondrial metabolic plasticity during hibernation could partly explain tissue-level hypoxia tolerance. My findings demonstrate greater anoxia tolerance in mitochondria isolated from ground squirrels during the hibernation season—especially during torpor—compared to SA squirrels. This mitochondrial anoxia tolerance likely contributes to the well-documented hypoxia-tolerant phenotype of multiple hibernator tissues.

Anoxia tolerance in these isolated mitochondria is likely associated with reduced oxidative stress upon re-oxygenation, as increasing the duration of anoxia from five to 30 mins did not further affect post-anoxic mitochondrial performance. I assessed maximal enzyme activity of three ETS complexes before and after anoxia to explain differences in performance, and the decreases in maximal activity that I report could have resulted from oxidative damage. Ideally, future studies could confirm this by measuring markers of oxidative stress (such as lipid peroxidation products, aconitase activity, GSSG:GSH ratios, protein carbonylation) and comparing these markers among groups. Unfortunately the small amount of sample recovered from respirometry experiments did not allow for such measurements to made in my study. Recently, fluorescent probes have been developed for the Oxygraph. These could be used to measure ROS production and O_2 consumption simultaneously in mitochondria before and after anoxic exposure, and compare rates between torpor, IBE and SA.

Following anoxia exposure, the increase in ST4 respiration in SA mitochondria was much greater compared with the other groups. To investigate mechanisms underlying this differential effect, immunoblot analysis of mitochondrial lysates could be performed to determine if UCP and ANT expression is elevated in mitochondria isolated from torpor animals. In addition, future respirometry experiments should inhibit UCPs and ANTs after anoxic exposure with GDP and CAT, respectively. If ST4 decreased significantly with the addition of these inhibitors, towards pre-anoxia levels, this would suggest that A/R stimulates ROS production which activates UCPs and ANTs, thereby uncoupling

respiration. If these inhibitors decrease ST4 only marginally, this would suggest increases in proton leak that are more consistent with damage to IMM phospholipids, perhaps due to a greater stimulation of ROS production. Regarding the putative role of UCPs in oxidative stress tolerance, it would be interesting to see whether addition of free-fatty acids, which activate UCPs, to mitochondria during anoxia could improve mitochondrial performance after re-oxygenation by inducing mild uncoupling and limiting ROS production.

Whether post-anoxia decreases in ST3 are the result of oxidative damage or regulatory modifications to mitochondrial enzymes during anoxia (e.g. reduced complex I capacity after S-nitrosylation) is unknown. In future experiments, ST3 should be measured initially after re-oxygenation, and 30 minutes after re-oxygenation, because a previous study determined that the inhibitory effects of S-nitrosylation on complex I can take 30 minutes to completely reverse (21). Also, the presence of post-translational modifications that are known to confer hypoxia tolerance (e.g. SUMOs, S-nitrosylation) should be compared among hibernation states to determine whether any modifications correlate with functional data.

My study demonstrates functional differences among hibernation states in their response to anoxia that may allow for tissue-level hypoxia tolerance in hibernators. My data also suggest mechanisms that may underlie these differences, developing hypotheses for further exploration. Although mitochondria are an important component of cellular and tissue metabolism, tolerance to anoxia and I/R involves both mitochondrial and extra-mitochondrial processes, so future studies should aim to repeat a similar design using whole cells to better represent the *in vivo* environment.

REFERENCES

1. **Acín-Pérez R**, **Fernández-Silva P**, **Peleato ML**, **Pérez-Martos A**, **Enriquez JA**. Respiratory active mitochondrial supercomplexes. *Mol Cell* 32: 529–539, 2008.

2. **Anderson EJ**, **Katunga LA**, **Willis MS**. Mitochondria as a source and target of lipid peroxidation products in healthy and diseased heart. *Clin Exp Pharmacol Physiol* 39: 179-193, 2012.

3. **Armstrong C**, **Staples JF**. The role of succinate dehydrogenase and oxaloacetate in metabolic suppression during hibernation and arousal. *J Comp Physiol B* 180: 775–783, 2010.

4. **Ascensao A**, **Magalhaes J**, **Soares JMC**, **Ferreira R**, **Neuparth MJ**, **Marques F**, **Oliveira P**, **Duarte JA**. Endurance training limits the functional alterations of heart rat mitochondria submitted to in vitro anoxia-reoxygenation. *Int J Cardiol* 109: 169–178, 2006.

5. **Barger JL**, **Brand MD**, **Barnes BM**, **Boyer BB**. Tissue-specific depression of mitochondrial proton leak and substrate oxidation in hibernating arctic ground squirrels. *Am J Physiol-Regul Integr Comp Physiol* 284: 1306–1313, 2003.

6. **Bickler PE**, **Buck LT**. Hypoxia tolerance in reptiles, amphibians, and fishes: life with variable oxygen availability. *Annu Rev Physiol* 69: 145–170, 2007.

7. **Boutilier RG**. Mechanisms of cell survival in hypoxia and hypothermia. *J Exp Biol* 204: 3171–3181, 2001.

8. **Brand MD**. Mitochondrial generation of superoxide and hydrogen peroxide as the source of mitochondrial redox signaling. *Free Radic Biol Med* 100: 14–31, 2016.

9. **Brand MD**. The proton leak across the mitochondrial inner membrane. *Biochim Biophys Acta BBA - Bioenerg* 1018: 128–133, 1990.

10. **Brand MD**, **Affourtit C**, **Esteves TC**, **Green K**, **Lambert AJ**, **Miwa S**, **Pakay JL**, **Parker N**. Mitochondrial superoxide: production, biological effects, and activation of uncoupling proteins. *Free Radic Biol Med* 37: 755–767, 2004.

11. **Brand MD**, **Chien L-F**, **Ainscow EK**, **Rolfe DFS**, **Porter RK**. The causes and functions of mitochondrial proton leak. *Biochim Biophys Acta BBA - Bioenerg* 1187: 132–139, 1994.

12. **Brand MD**, **Chien L-F**, **Diolez P**. Experimental discrimination between proton leak and redox slip during mitochondrial electron transport. *Biochem J* 297: 27–29, 1994.

13. **Brand MD**, **Nicholls DG**. Assessing mitochondrial dysfunction in cells. *Biochem J* 435: 297–312, 2011.

14. **Brown GC**, **Cooper CE**. *Bioenergetics: A Practical Approach*. Oxford, UK: IRL Press, 1995.

15. **Bullard RW**, **Funkhouser GE**. Estimated regional blood flow by rubidium 86 distribution during arousal from hibernation. *Am J Physiol-Leg Content* 203: 266–270, 1962.

16. **Cao W**, **Carney JM**, **Duchon A**, **Floyd RA**, **Chevion M**. Oxygen free radical involvement in ischemia and reperfusion injury to brain. *Neurosci Lett* 88: 233–238, 1988.

17. **Carey HV**, **Frank CL**, **Seifert JP**. Hibernation induces oxidative stress and activation of NF-κB in ground squirrel intestine. *J Comp Physiol B* 170: 551–559, 2000.

18. **Carey HV**, **Rhoads CA**, **Aw TY**. Hibernation induces glutathione redox imbalance in ground squirrel intestine. *J Comp Physiol B* 173: 269–276, 2003.

19. **Chen Q**, **Camara AKS**, **Stowe DF**, **Hoppel CL**, **Lesnefsky EJ**. Modulation of electron transport protects cardiac mitochondria and decreases myocardial injury during ischemia and reperfusion. *Am J Physiol-Cell Physiol* 292: 137–147, 2007.

20. **Chen Q**, **Moghaddas S**, **Hoppel CL**, **Lesnefsky EJ**. Reversible blockade of electron transport during ischemia protects mitochondria and decreases myocardial injury following reperfusion. *J Pharmacol Exp Ther* 319: 1405–1412, 2006.

21. **Chouchani ET**, **Methner C**, **Nadtochiy SM**, **Logan A**, **Pell VR**, **Ding S**, **James AM**, **Cochemé HM**, **Reinhold J**, **Lilley KS**, **Partridge L**, **Fearnley IM**, **Robinson AJ**, **Hartley RC**, **Smith RAJ**, **Krieg T**, **Brookes PS**, **Murphy MP**. Cardioprotection by S-nitrosation of a cysteine switch on mitochondrial complex I. *Nat Med* 19: 753–759, 2013.

22. **Chung D**, **Lloyd GP**, **Thomas RH**, **Guglielmo CG**, **Staples JF**. Mitochondrial respiration and succinate dehydrogenase are suppressed early during entrance into a hibernation bout, but membrane remodeling is only transient. *J Comp Physiol B* 181: 699–711, 2011.

23. **Cole-Ezea P**, **Swan D**, **Shanley D**, **Hesketh J**. Glutathione peroxidase 4 has a major role in protecting mitochondria from oxidative damage and maintaining oxidative phosphorylation complexes in gut epithelial cells. *Free Radic Biol Med* 53: 488–497, 2012.

24. **D'Alessandro A**, **Nemkov T**, **Bogren LK**, **Martin SL**, **Hansen KC**. Comfortably numb and back: plasma metabolomics reveals biochemical adaptations in the hibernating 13-lined ground squirrel. *J Proteome Res* 16: 958–969, 2017.

25. **Dave KR**, **Prado R**, **Raval AP**, **Drew KL**, **Perez-Pinzon MA**. The Arctic ground squirrel brain is resistant to injury from cardiac arrest during euthermia. *Stroke* 37: 1261–1265, 2006.

26. **Du G**, **Mouithys-Mickalad A**, **Sluse FE**. Generation of superoxide anion by mitochondria and impairment of their functions during anoxia and reoxygenation in vitro. *Free Radic Biol Med* 25: 1066–1074, 1998.

27. **Elrod JW**, **Calvert JW**, **Morrison J**, **Doeller JE**, **Kraus DW**, **Tao L**, **Jiao X**, **Scalia R**, **Kiss L**, **Szabo C**, **Kimura H**, **Chow C-W**, **Lefer DJ**. Hydrogen sulfide attenuates myocardial ischemia-reperfusion injury by preservation of mitochondrial function. *Proc Natl Acad Sci* 104: 15560–15565, 2007.

28. **Finichiu PG**, **Larsen DS**, **Evans C**, **Larsen L**, **Bright TP**, **Robb EL**, **Trnka J**, **Prime TA**, **James AM**, **Smith RAJ**, **Murphy MP**. A mitochondria-targeted derivative of ascorbate: MitoC. *Free Radic Biol Med* 89: 668–678, 2015.

29. **Galli GLJ**, **Lau GY**, **Richards JG**. Beating oxygen: chronic anoxia exposure reduces mitochondrial F1FO-ATPase activity in turtle (*Trachemys scripta*) heart. *J Exp Biol* 216: 3283–3293, 2013.

30. **Galli GLJ**, **Richards JG**. Mitochondria from anoxia-tolerant animals reveal common strategies to survive without oxygen. *J Comp Physiol B* 184: 285–302, 2014.

31. **Gaschler MM**, **Stockwell BR**. Lipid peroxidation in cell death. *Biochem Biophys Res Commun* 482: 419–425, 2017.

32. **Geiser F**. Metabolic rate and body temperature reduction during hibernation and daily torpor. *Annu Rev Physiol* 66: 239–274, 2004.

33. **Gerson AR**, **Brown JCL**, **Thomas R**, **Bernards MA**, **Staples JF**. Effects of dietary polyunsaturated fatty acids on mitochondrial metabolism in mammalian hibernation. *J Exp Biol* 211: 2689–2699, 2008.

34. **Halestrap AP**. The regulation of the matrix volume of mammalian mitochondria in vivo and in vitro and its role in the control of mitochondrial metabolism. *Biochim Biophys Acta BBA - Bioenerg* 973: 355–382, 1989.

35. **Halestrap AP**, **Clarke SJ**, **Javadov SA**. Mitochondrial permeability transition pore opening during myocardial reperfusion—a target for cardioprotection. *Cardiovasc Res* 61: 372–385, 2004.

36. **Ham A-JL**, **Liebler DC**. Vitamin E oxidation in rat liver mitochondria. *Biochemistry* 34: 5754–5761, 1995.

37. **Hayes JP**. Field and maximal metabolic rates of deer mice (*Peromyscus maniculatus*) at low and high altitudes. *Physiol Zool* 62: 732–744, 1989.

38. **Hermes-Lima M**, **Zenteno-Savín T**. Animal response to drastic changes in oxygen availability and physiological oxidative stress. *Comp Biochem Physiol Part C Toxicol Pharmacol* 133: 537–556, 2002.

39. **Hickey AJR**, **Renshaw GMC**, **Speers-Roesch B**, **Richards JG**, **Wang Y**, **Farrell AP**, **Brauner CJ**. A radical approach to beating hypoxia: depressed free radical release from heart fibres of the hypoxia-tolerant epaulette shark *Hemiscyllum ocellatum*. *J Comp Physiol B* 182: 91–100, 2012.

40. **Hillenius WJ**, **Ruben JA**. The evolution of endothermy in terrestrial vertebrates: who? when? why? *Physiol Biochem Zool* 77: 1019–1042, 2004.

41. **Hochachka PW**, **Guppy M**. *Metabolic Arrest and the Control of Biological Time*. Harvard University Press, 1987.

42. **Imai H**, **Nakagawa Y**. Biological significance of phospholipid hydroperoxide glutathione peroxidase (PHGPx, GPx4) in mammalian cells. *Free Radic Biol Med* 34: 145–169, 2003.

43. **Jastroch M**, **Divakaruni AS**, **Mookerjee S**, **Treberg JR**, **Brand MD**. Mitochondrial proton and electron leaks. *Essays Biochem* 47: 53–67, 2010.

44. **Kirby DM**, **Thorburn DR**, **Turnbull DM**, **Taylor RW**. Biochemical assays of respiratory chain complex activity. *Methods Cell Biol* 80: 93–119, 2007.

45. **Kolomiytseva IK**, **Perepelkina NI**, **Fesenko EE**. Lipids of liver membrane structures during hibernation of the arctic ground squirrel *Spermophilus undulatus*. *Dokl Biochem Biophys* 448: 15–18, 2013.

46. **Kurtz CC**, **Lindell SL**, **Mangino MJ**, **Carey HV**. Hibernation confers resistance to intestinal ischemia-reperfusion injury. *Am J Physiol-Gastrointest Liver Physiol* 291: 895–901, 2006.

47. **Lee Y**, **Miyake S**, **Wakita H**, **McMullen DC**, **Azuma Y**, **Auh S**, **Hallenbeck JM**. Protein SUMOylation is massively increased in hibernation torpor and is critical for the cytoprotection provided by ischemic preconditioning and hypothermia in SHSY5Y cells. *J Cereb Blood Flow Metab* 27: 950–962, 2007.

48. **Li P**, **Zhang D**, **Shen L**, **Dong K**, **Wu M**, **Ou Z**, **Shi D**. Redox homeostasis protects mitochondria through accelerating ROS conversion to enhance hypoxia resistance in cancer cells. *Sci Rep* 6: 22831, 2016.

49. **Lindell SL**, **Klahn SL**, **Piazza TM**, **Mangino MJ**, **Torrealba JR**, **Southard JH**, **Carey HV**. Natural resistance to liver cold ischemia-reperfusion injury associated with the hibernation phenotype. *Am J Physiol-Gastrointest Liver Physiol* 288: 473–480, 2005.

50. **Lipton P**. Ischemic cell death in brain neurons. *Physiol Rev* 79: 1431–1568, 1999.

51. **Ma YL**, **Zhu X**, **Rivera PM**, **Tøien Ø**, **Barnes BM**, **LaManna JC**, **Smith MA**, **Drew KL**. Absence of cellular stress in brain after hypoxia induced by arousal from hibernation in Arctic ground squirrels. *Am J Physiol-Regul Integr Comp Physiol* 289: 1297–1306, 2005.

52. **Mathers K**. Regulation of liver mitochondrial metabolism during hibernation by post-translational modification. *Electron. Thesis Diss. Repos.* 5098, 2017. https://ir.lib.uwo.ca/etd/5098.

53. **Mathers KE**, **McFarlane SV**, **Zhao L**, **Staples JF**. Regulation of mitochondrial metabolism during hibernation by reversible suppression of electron transport system enzymes. *J Comp Physiol B* 187: 227–234, 2017.

54. **Mookerjee SA**, **Divakaruni AS**, **Jastroch M**, **Brand MD**. Mitochondrial uncoupling and lifespan. *Mech Ageing Dev* 131: 463–472, 2010.

55. **Murphy MP**, **Holmgren A**, **Larsson N-G**, **Halliwell B**, **Chang CJ**, **Kalyanaraman B**, **Rhee SG**, **Thornalley PJ**, **Partridge L**, **Gems D**, **Nyström T**, **Belousov V**, **Schumacker PT**, **Winterbourn CC**. Unraveling the biological roles of reactive oxygen species. *Cell Metab* 13: 361–366, 2011.

56. **Nadtochiy SM**, **Tompkins AJ**, **Brookes PS**. Different mechanisms of mitochondrial proton leak in ischaemia/reperfusion injury and preconditioning: implications for pathology and cardioprotection. *Biochem J* 395: 611–618, 2006.

57. **Nicholls DG**, **Ferguson, Stuart J.** *Bioenergetics*. Fourth Edition. London, UK: Academic Press, 2013.

58. **Ou J**, **Ball JM**, **Luan Y**, **Zhao T**, **Miyagishima KJ**, **Xu Y**, **Zhou H**, **Chen J**, **Merriman DK**, **Xie Z**, **Mallon BS**, **Li W**. iPSCs from a hibernator provide a platform for studying cold adaptation and its potential medical applications. *Cell* 173: 851-863, 2018.

59. **Page MM**, **Peters CW**, **Staples JF**, **Stuart JA**. Intracellular antioxidant enzymes are not globally upregulated during hibernation in the major oxidative tissues of the 13-lined ground squirrel *Spermophilus tridecemlineatus*. *Comp Biochem Physiol A Mol Integr Physiol* 152: 115–122, 2009.

60. **Paradies G**, **Paradies V**, **De Benedictis V**, **Ruggiero FM**, **Petrosillo G**. Functional role of cardiolipin in mitochondrial bioenergetics. *Biochim Biophys Acta BBA - Bioenerg* 1837: 408–417, 2014.

61. **Park TJ**, **Reznick J**, **Peterson BL**, **Blass G**, **Omerbašić D**, **Bennett NC**, **Kuich PHJL**, **Zasada C**, **Browe BM**, **Hamann W**, **Applegate DT**, **Radke MH**, **Kosten T**, **Lutermann H**, **Gavaghan V**, **Eigenbrod O**, **Bégay V**, **Amoroso VG**, **Govind V**, **Minshall RD**, **Smith ESJ**, **Larson J**, **Gotthardt M**, **Kempa S**, **Lewin GR**. Fructose-driven glycolysis supports anoxia resistance in the naked mole-rat. *Science* 356: 307–311, 2017.

62. **Peralta C**, **Hotter G**, **Closa D**, **Prats N**, **Xaus C**, **Gelpí E**, **Roselló-Catafau J**. The protective role of adenosine in inducing nitric oxide synthesis in rat liver ischemia preconditioning is mediated by activation of adenosine A2 receptors. *Hepatology* 29: 126–132, 1999.

63. **Petit PX**, **O'connor JE**, **Grunwald D**, **Brown SC**. Analysis of the membrane potential of rat- and mouse-liver mitochondria by flow cytometry and possible applications. *Eur J Biochem* 194: 389–397, 1990.

64. **Pfeiffer K**, **Gohil V**, **Stuart RA**, **Hunte C**, **Brandt U**, **Greenberg ML**, **Schägger H**. Cardiolipin stabilizes respiratory chain supercomplexes. *J Biol Chem* 278: 52873–52880, 2003.

65. **Piantadosi CA**, **Zhang J**. Mitochondrial generation of reactive oxygen species after brain ischemia in the rat. *Stroke* 27: 327–332, 1996.

66. **Powell CS**, **Jackson RM**. Mitochondrial complex I, aconitase, and succinate dehydrogenase during hypoxia-reoxygenation: modulation of enzyme activities by MnSOD. *Am J Physiol-Lung Cell Mol Physiol* 285: 189–198, 2003.

67. **Revsbech IG**, **Fago A**. Regulation of blood oxygen transport in hibernating mammals. *J Comp Physiol B* 187: 847–856, 2017.

68. **Revsbech IG**, **Shen X**, **Chakravarti R**, **Jensen FB**, **Thiel B**, **Evans AL**, **Kindberg J**, **Fröbert O**, **Stuehr DJ**, **Kevil CG**, **Fago A**. Hydrogen sulfide and nitric oxide metabolites in the blood of free-ranging brown bears and their potential roles in hibernation. *Free Radic Biol Med* 73: 349–357, 2014.

69. **Rose JC**, **Epperson LE**, **Carey HV**, **Martin SL**. Seasonal liver protein differences in a hibernator revealed by quantitative proteomics using whole animal isotopic labeling. *Comp Biochem Physiol Part D Genomics Proteomics* 6: 163–170, 2011.

70. **Rouslin W**, **Ranganathan S**. Impaired function of mitochondrial electron transfer complex I in canine myocardial ischemia: Loss of flavin mononucleotide. *J Mol Cell Cardiol* 15: 537–542, 1983.

71. **Russell RL**, **O'Neill PH**, **Epperson LE**, **Martin SL**. Extensive use of torpor in 13-lined ground squirrels in the fall prior to cold exposure. *J Comp Physiol B* 180: 1165–1172, 2010.

72. **Serkova NJ**, **Rose JC**, **Epperson LE**, **Carey HV**, **Martin SL**. Quantitative analysis of liver metabolites in three stages of the circannual hibernation cycle in 13-lined ground squirrels by NMR. *Physiol Genomics* 31: 15–24, 2007.

73. **Sheriff MJ**, **Williams CT**, **Kenagy GJ**, **Buck CL**, **Barnes BM**. Thermoregulatory changes anticipate hibernation onset by 45 days: data from free-living arctic ground squirrels. *J Comp Physiol B* 182: 841–847, 2012.

74. **Shiva S**, **Sack MN**, **Greer JJ**, **Duranski M**, **Ringwood LA**, **Burwell L**, **Wang X**, **MacArthur PH**, **Shoja A**, **Raghavachari N**, **Calvert JW**, **Brookes PS**, **Lefer DJ**, **Gladwin MT**. Nitrite augments tolerance to ischemia/reperfusion injury via the modulation of mitochondrial electron transfer. *J Exp Med* 204: 2089–2102, 2007.

75. **Singer D**. Neonatal tolerance to hypoxia: a comparative-physiological approach. *Comp Biochem Physiol A Mol Integr Physiol* 123: 221–234, 1999.

76. **Staples JF**. Metabolic suppression in mammalian hibernation: the role of mitochondria. *J Exp Biol* 217: 2032–2036, 2014.

77. **Staples JF**. Metabolic Flexibility: Hibernation, Torpor, and Estivation. *Compr Physiol* 6: 737–771, 2016.

78. **Storz JF**, **McClelland GB**. Rewiring metabolism under oxygen deprivation. *Science* 356: 248–249, 2017.

79. **Strumwasser F**. Factors in the pattern, timing and predictability of hibernation in the squirrel, *Citellus beecheyi*. *Am J Physiol-Leg Content* 196: 8–14, 1958.

80. **Sun J**, **Nguyen T**, **Aponte AM**, **Menazza S**, **Kohr MJ**, **Roth DM**, **Patel HH**, **Murphy E**, **Steenbergen C**. Ischaemic preconditioning preferentially increases protein S-nitrosylation in subsarcolemmal mitochondria. *Cardiovasc Res* 106: 227–236, 2015.

81. **Takaki M**, **Nakahara H**, **Kawatani Y**, **Utsumi K**, **Suga H**. No suppression of respiratory function of mitochondria isolated from the hearts of anesthetized rats with high-dose pentobarbital sodium. *Jpn J Physiol* 47: 87–92, 1997.

82. **Tøien Ø**, **Drew KL**, **Chao ML**, **Rice ME**. Ascorbate dynamics and oxygen consumption during arousal from hibernation in Arctic ground squirrels. *Am J Physiol-Regul Integr Comp Physiol* 281: R572–R583, 2001.

83. **Van der Paal J**, **C. Neyts E**, **W. Verlackt CC**, **Bogaerts A**. Effect of lipid peroxidation on membrane permeability of cancer and normal cells subjected to oxidative stress. *Chem Sci* 7: 489–498, 2016.

84. **Van Breukelen F**, **Krumschnabel G**, **Podrabsky JE**. Vertebrate cell death in energy-limited conditions and how to avoid it: what we might learn from mammalian hibernators and other stress-tolerant vertebrates. *Apoptosis* 15: 386–399, 2010.

85. **Van Breukelen F**, **Martin SL**. The hibernation continuum: Physiological and molecular aspects of metabolic plasticity in mammals. *Physiology* 30: 273–281, 2015.

86. **Vaughan DK**, **Gruber AR**, **Michalski ML**, **Seidling J**, **Schlink S**. Capture, care, and captive breeding of 13-lined ground squirrels, *Spermophilus tridecemlineatus*. *Lab Anim* 35: 33-40, 2006.

87. **Vogt FD**, **Lynch GR**. Influence of ambient temperature, nest availability, huddling, and daily torpor on energy expenditure in the white-footed mouse *Peromyscus leucopus*. *Physiol Zool* 55: 56–63, 1982.

88. **Walters AM**, **Porter GA**, **Brookes PS**. Mitochondria as a drug target in ischemic heart disease and cardiomyopathy. *Circ Res* 111: 1222–1236, 2012.

89. **Wilkinson KA**, **Henley JM**. Mechanisms, regulation and consequences of protein SUMOylation. *Biochem J* 428: 133–145, 2010.

90. **Wong H-S**, **Dighe PA**, **Mezera V**, **Monternier P-A**, **Brand MD**. Production of superoxide and hydrogen peroxide from specific mitochondrial sites under different bioenergetic conditions. *J Biol Chem* 292: 16804–16809, 2017.

91. **Wong-ekkabut J**, **Xu Z**, **Triampo W**, **Tang I-M**, **Peter Tieleman D**, **Monticelli L**. Effect of lipid peroxidation on the properties of lipid bilayers: A molecular dynamics study. *Biophys J* 93: 4225–4236, 2007.

92. **Yellon DM**, **Downey JM**. Preconditioning the myocardium: From cellular physiology to clinical cardiology. *Physiol Rev* 83: 1113–1151, 2003.

APPENDIX

Appendix 1. Animal use ethics approval

eSirius3G -- 2012-016 Continuing Review Approved

Subject: eSirius3G -- 2012-016 Continuing Review Approved
From:
Date: 01/08/2017 1:02 PM
To:

Western

2012-016:5:

AUP Number: 2012-016
AUP Title: Regulation of mitochondrial metabolism in mammalian hibernation and ageing.
Yearly Renewal Date: 08/05/2016

The YEARLY RENEWAL to Animal Use Protocol (AUP) 2012-016 has been approved by the Animal Care Committee (ACC), and will be approved for one year following the above review date.

Please at this time review your AUP with your research team to ensure full understanding by everyone listed within this AUP.

As per your declaration within this approved AUP, you are obligated to ensure that:

1) Animals used in this research project will be cared for in alignment with:
   a) Western's Senate MAPPs 7.12, 7.10, and 7.15
   http://www.uwo.ca/univsec/policies_procedures/research.html
   b) University Council on Animal Care Policies and related Animal Care Committee procedures
   http://uwo.ca/research/services/animalethics/animal_care_and_use_policies.html
2) As per UCAC's Animal Use Protocols Policy,
   a) this AUP accurately represents intended animal use;
   b) external approvals associated with this AUP, including permits and scientific/departmental peer approvals, are complete and accurate;
   c) any divergence from this AUP will not be undertaken until the related Protocol Modification is approved by the ACC; and
   d) AUP form submissions - Annual Protocol Renewals and Full AUP Renewals - will be submitted
   and attended to within timeframes outlined by the ACC. http://uwo.ca/research/services/animalethics/animal_use_protocols.html
3) As per MAPP 7.10 all individuals listed within this AUP as having any hands-on animal contact will
   a) be made familiar with and have direct access to this AUP;
   b) complete all required CCAC mandatory training (_training@uwo.ca); and
   c) be overseen by me to ensure appropriate care and use of animals.
4) As per MAPP 7.15,
   a) Practice will align with approved AUP elements;
   b) Unrestricted access to all animal areas will be given to ACVS Veterinarians and ACC Leaders;
   c) UCAC policies and related ACC procedures will be followed, including but not limited to:
      i) Research Animal Procurement
      ii) Animal Care and Use Records
      iii) Sick Animal Response
      iv) Continuing Care Visits
5) As per institutional OH&S policies, all individuals listed within this AUP who will be using or potentially exposed to hazardous materials will have completed in advance the appropriate institutional OH&S training, facility-level training, and reviewed related (M)SDS Sheets, http://www.uwo.ca/hr/learning/required/index.html

Submitted by: Copeman, Laura
on behalf of the Animal Care Committee
University Council on Animal Care

The University of Western Ontario

Appendix 2. Mean absolute respiration rates of all groups

Performance Metric	Group			
	Torpor	IBE	Summer	Rat
$ST3_i$	79.15±6.44	112±6.01	121±8.44	47.4±7.77
$ST3_a$	59.2±6.19	60.4±4.27	68.4±9.59	28.04±4.27
$ST4_i$	33.2±3.88	24.0±3.96	20.3±3.70	6.72±0.89
$ST4_a$	39.6±4.93	29.6±4.05	47.7±3.03	18.99±1.31

Values are mean ± SE (nmol O_2 min^{-1} ml^{-1} mg $protein^{-1}$). ST3=State 3, ST4=State 4, i = initial, a = post-anoxia

Appendix 3. Interaction plots of complex I- and II-linked maximal respiration (A) and leak respiration (B) of liver mitochondria before and after 30 minutes of anoxia. Data are presented as mean ± SE for N=6 torpor N=6 IBE and N=8 summer samples. These data were analyzed paired t-tests. In ST3 (A) anoxia had a significant effect on IBE (*, t_5=6.65, P=0.001) and summer mitochondria (*, t_7=4.18, P=0.004) but no effect on torpor (t_5=0.64, P=0.55). In ST4 (B) anoxia had a significant effect on all groups (†, torpor: t_5=3.36, P=0.02; IBE: t_5=11.05, P=0.0001; SA: t_7=2.93, P=0.022).

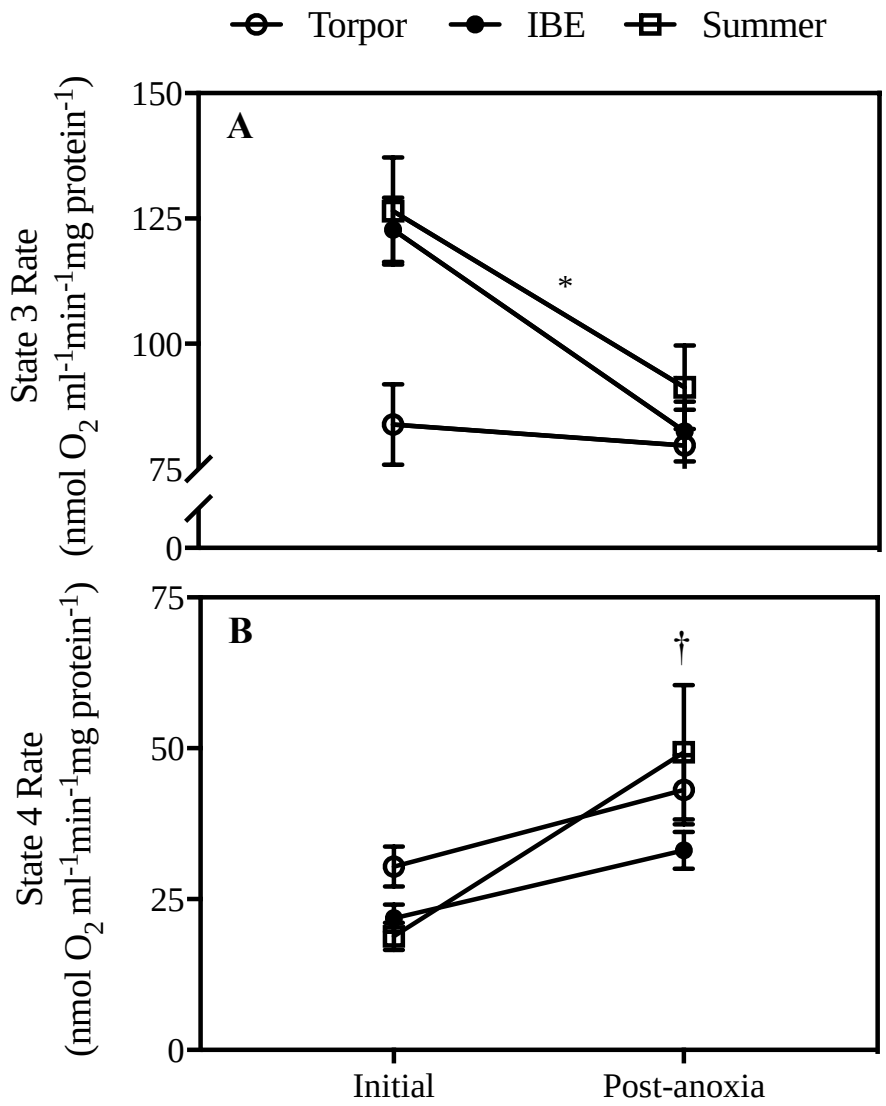

CURRICULUM VITAE

Name	Leah Hayward
Post-secondary Education and Degrees	The University of Western Ontario London, Ontario, Canada 2018 M.Sc.
	McMaster University Hamilton, Ontario, Canada 2012-2016 B.Sc.
Scholarships	Queen Elizabeth II Graduate Scholarship in Science and Technology 2016
Awards	Runner-up: Canadian Society of Zoologists Helen I. Battle Award for Best Student Poster 2018
	Biology Graduate Travel Award 2018
	McMaster University Senate Scholarship 2014

Presentations

Hayward, L., Mathers, K., and Staples, J. (2018) Anoxia-reoxygenation does not alter mitochondrial function in ground squirrels during hibernation. The 2018 American Physiological Society Intersociety Meeting on Comparative Physiology. New Orleans, LA.

Hayward, L., Mathers, K., and Staples, J. (2018) Hibernation protects mitochondria from *in vitro* anoxic exposure. Society for Experimental Biology Annual Meeting. Firenze, IT.

Hayward, L., Mathers, K., and Staples, J. (2018) The Effect of Anoxia on Mitochondrial Performance in a Hibernator (*Ictidomys tridecemlineatus*). 57th Annual Meeting of the Canadian Society of Zoologists. Memorial University, St. John's, NFLD.

Hayward, L., Mathers, K., and Staples, J. (2017) The role of mitochondria in hypoxia tolerance of hibernators. 56th Annual Meeting of the Canadian Society of Zoologists. The University of Manitoba, Winnipeg, MB.